P-07-138

Forsmark site investigation

Formation factor logging in situ by electrical methods in KFM01D and KFM08C

Martin Löfgren, Kemakta Konsult AB

August 2007

Svensk Kärnbränslehantering AB
Swedish Nuclear Fuel
and Waste Management Co
Box 5864
SE-102 40 Stockholm Sweden
Tel 08-459 84 00
+46 8 459 84 00
Fax 08-661 57 19
+46 8 661 57 19

ISSN 1651-4416
SKB P-07-138

Forsmark site investigation

Formation factor logging in situ by electrical methods in KFM01D and KFM08C

Martin Löfgren, Kemakta Konsult AB

August 2007

Keywords: AP PF 400-06-099, In situ, Formation factor, Rock resistivity, Electrical conductivity.

Abstract

This report presents measurements and interpretations of the formation factor of the rock surrounding the boreholes KFM01D and KFM08C in Forsmark, Sweden. The formation factor was logged in situ by electrical methods.

For KFM01D, the in situ rock matrix formation factors obtained range from $1.9 \cdot 10^{-5}$ to $2.1 \cdot 10^{-4}$. The in situ fractured rock formation factors obtained range from $1.9 \cdot 10^{-5}$ to $6.6 \cdot 10^{-4}$. The obtained formation factor distributions correspond fairly well with the log-normal distribution. The mean values and standard deviations of the obtained $\log_{10}$-normal distributions are –4.49 and 0.094, and –4.45 and 0.15 for the in situ rock matrix and fractured rock formation factor, respectively. The small variance for the rock matrix formation factor should be noted.

For KFM08C, the in situ rock matrix formation factors obtained range from $9.3 \cdot 10^{-6}$ to $3.6 \cdot 10^{-4}$. The in situ fractured rock formation factors obtained range from $8.4 \cdot 10^{-6}$ to $2.2 \cdot 10^{-3}$. The distributions of the formation factors are fairly well described by the log-normal distribution. The mean values and standard deviations of the obtained $\log_{10}$-normal distributions are –4.46 and 0.13, and –4.39 and 0.20 for the in situ rock matrix and fractured rock formation factor, respectively. The small variance for the rock matrix formation factor should be noted. The only laboratory (rock matrix) formation factor obtained from a single drill core sample had the value $2.09 \cdot 10^{-4}$.

When obtaining the electrical conductivity profiles of the groundwater in the boreholes, complementary data from matrix fluid measurements on drill core samples were used.

Sammanfattning

Denna rapport presenterar mätningar och tolkningar av bergets formationsfaktor runt borrhålen KFM01D och KFM08C i Forsmark, Sverige. Formationsfaktorn har loggats in situ med elektriska metoder.

För KFM01D varierar den erhållna in situ formationsfaktorn för bergmatrisen från $1{,}9 \cdot 10^{-5}$ till $2{,}1 \cdot 10^{-4}$. Den erhållna in situ formationsfaktorn för sprickigt berg varierar från $1{,}9 \cdot 10^{-5}$ till $6{,}6 \cdot 10^{-4}$. De erhållna formationsfaktordistributionerna beskrivs relativt väl av log-normal fördelningen. Medelvärdena och standardavvikelserna för de erhållna $\log_{10}$-normalfördelningarna är –4,49 och 0,094 samt –4,45 och 0,15 för in situ formationsfaktorn för bergmatrisen respektive sprickigt berg. Den begränsade variansen för formationsfaktorn för bergmatrisen bör noteras.

För KFM08C varierar den erhållna in situ formationsfaktorn för bergmatrisen från $9{,}3 \cdot 10^{-6}$ till $3{,}6 \cdot 10^{-4}$. Den erhållna in situ formationsfaktorn för sprickigt berg varierar från $8{,}4 \cdot 10^{-6}$ till $2{,}2 \cdot 10^{-3}$. De erhållna formationsfaktordistributionerna beskrivs relativt väl av log-normal fördelningen. Medelvärdena och standardavvikelserna för de erhållna $\log_{10}$-normalfördelningarna är –4,46 och 0,13 samt –4,39 och 0,20 för in situ formationsfaktorn för bergmatrisen respektive sprickigt berg. Den begränsade variansen för formationsfaktorn för bergmatrisen bör noteras. En enda formationsfaktor (för bergmatrisen) erhölls i laboratoriet, på ett enda borrkärneprov, med värdet $2{,}09 \cdot 10^{-4}$.

För att erhålla profiler över grundvattnets elektriska konduktivitet i borrhålen användes kompletterande data från matrisporvattenmätningar.

Contents

1 Introduction

This document reports the data gained from measurements of the formation factor of rock surrounding the boreholes KFM01D and KFM08C, within the site investigation at Forsmark. A comparison is made with a formation factor obtained in the laboratory on a single sample from the drill core of KFM08C. The work was carried out in accordance with Activity Plan AP PF 400-06-099. In Table 1-1, controlling documents for performing this activity are listed. Both Activity Plan and Method Description are SKB's internal controlling documents.

The formation factor was logged by electrical methods. Other contractors performed the field-work and laboratory work, which is outside the framework of this activity. The interpretation of in situ data and compilation of formation factor logs were performed by Kemakta Konsult AB in Stockholm, Sweden.

Figure 1-1 shows the Forsmark site investigation area and the locations of some of the different drill sites. KFM01D and KFM08C are located at the drill sites DS1 and DS8, respectively.

Table 1-1. Controlling documents for performance of the activity.

Activity plan	**Number**	**Version**
Bestämning av formationsfaktorn från in situ resistivitetsmätningar i KFM01D och KFM06C*	AP PF 400-06-099	1.0
Method descriptions	**Number**	**Version**
Bestämning av formationsfaktorn med elektriska metoder	SKB MD 530.007	1.0

*The AP was initially intended for work on KFM06C, which was in a later stage changed to KFM08C.

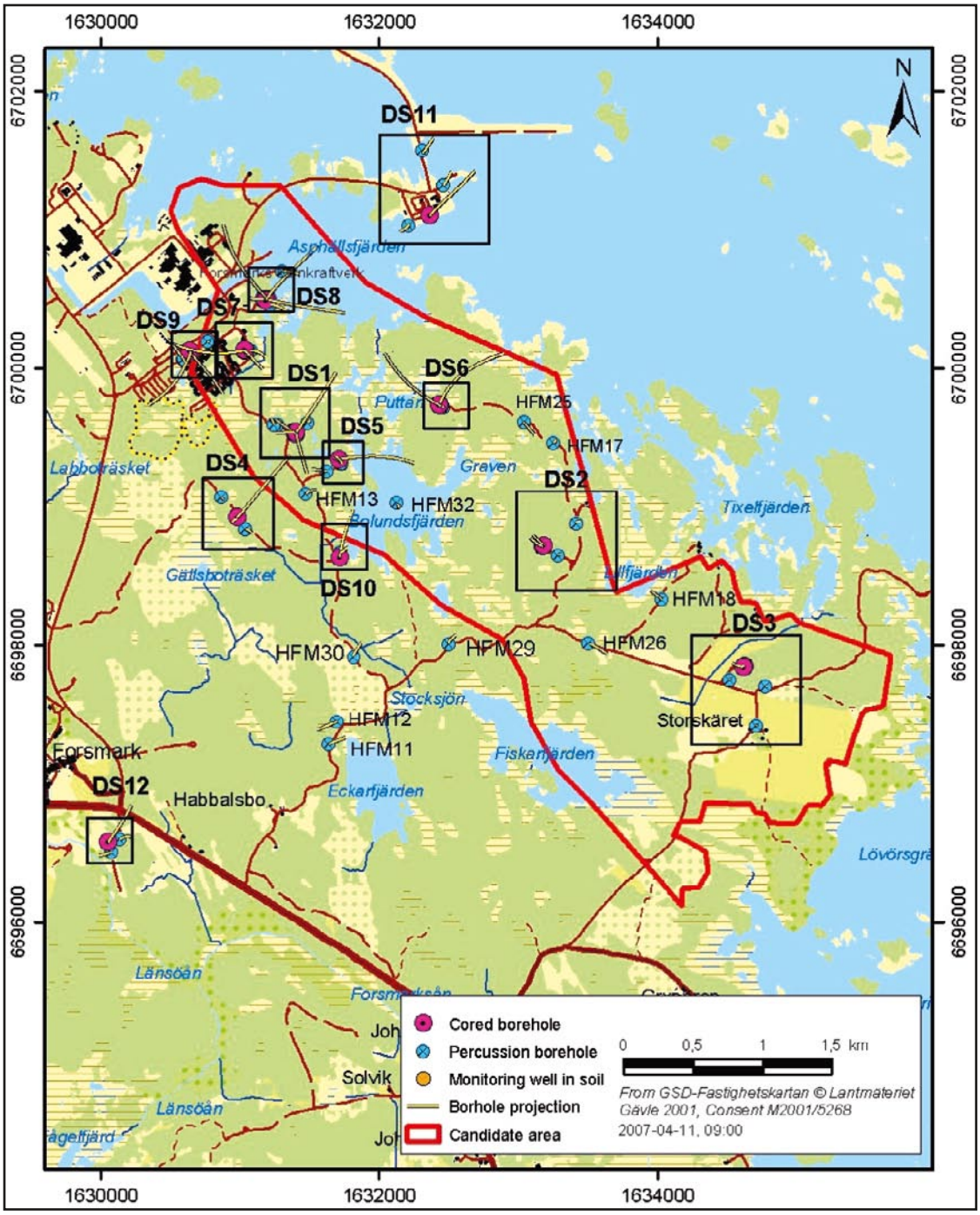

Figure 1-1. *General overview over the Forsmark site investigation area.*

2 Objective and scope

The formation factor is an important parameter that may be used directly in safety assessment calculations of radionuclide transport in crystalline rock. The main objective of this work is to obtain the formation factor of the rock mass surrounding the boreholes KFM01D and KFM08C. This has been achieved by performing formation factor loggings by electrical methods in situ. The in situ method gives a great number of formation factors obtained under more natural conditions than in the laboratory. To obtain the in situ formation factor, results from previous loggings were used. A formation factor from a single drill core sample of KFM08C has previously been obtained and a comparison with this formation factor is made. Other contractors carried out the fieldwork and laboratory work.

3 Equipment

3.1 Rock resistivity measurements

The resistivity of the rock surrounding the boreholes KFM01D /1/ and KFM08C /2/ was logged using the focused rock resistivity tool Century 9072. The tool emits an alternating current perpendicular to the borehole axis from a main current electrode. The shape of the current field is controlled by electric fields emitted by guard electrodes. By using a focused tool, the disturbance from the borehole is minimised. The quantitative measuring range of the Century 9072 tool is 0–50,000 ohm.m according to the manufacturer. In the site investigations the rock resistivity may also be logged using the Century 9030 tool. However, this tool may not be suitable for quantitative logging in granitic rock and the results are not used in this report.

3.2 Groundwater electrical conductivity measurements

The EC (electrical conductivity) of the borehole fluid in KFM01D /3/ and KFM08C /4/ was logged using the POSIVA difference flow meter. The tool is shown in Figure 3-1.

When logging the EC of the borehole fluid, the lower rubber disks of the tool are not used. During the measurements, a drawdown can either be applied or not. Measurements were carried out before and after extensive pumping in boreholes KFM01D and KFM08C.

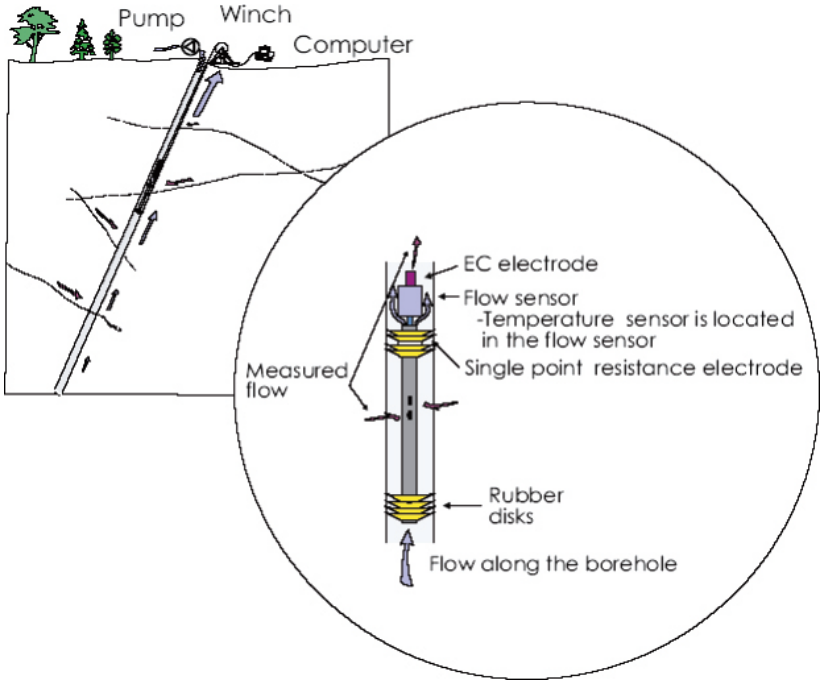

Figure 3-1. *Schematics of the POSIVA difference flow meter (image taken from /3/).*

When using both the upper and the lower rubber disks, a section around a specific fracture can be packed off. By applying a drawdown at the surface, groundwater can thus be extracted from specific fractures. This is done in fracture specific EC measurements. By also measuring the groundwater flow out of the fracture, it is calculated how long time it will take to fill up the packed off borehole section three times. During this time the EC is measured and a transient EC curve is obtained. After this time it is assumed that the measured EC is representative for the groundwater flowing out of the fracture. The measurements may be disturbed by leakage of borehole fluid into the packed off section and development of gas from species dissolved in the groundwater. Interpretations of transient EC curves are discussed in /5/. The quantitative measuring range of the EC electrode of the POSIVA difference flow meter is 0.02–11 S/m.

The EC, among other entities, of the groundwater coming from fractures in larger borehole sections is measured as a part of the hydrochemical characterisation using the Chemmac equipment. A section is packed off and by applying a drawdown, groundwater is extracted from fractures within the section and brought to the surface for chemical analysis. Complete hydrochemical characterisation was performed in KFM01D /6/. In addition to using the Chemmac equipment, so called SLT sampling and PSS sampling were also performed in KFM01D /6/. The SLT sampling was performed on fractures of low transmissivity. In the SLT sampling, the hydraulic gradient needed to withdraw groundwater is created by applying an under pressure in a 1 m long packed off section for a short period of time (a few minutes up to a few hours) and sampling the water that has flown into the section. In the PSS sampling, the Pipe String System, that is generally used for hydraulic injection tests, was used for withdrawing water. In this measurement the packed off section was 5 m long /6/.

3.3 Difference flow loggings

By using the POSIVA difference flow meter, water-conducting fractures can be located. The tool, shown in Figure 3-1, has a flow sensor and the flow from fractures in packed off sections can be measured. When performing these measurements, both the upper and the lower rubber disks are used. Measurements can be carried out both with and without applying a drawdown. The quantitative measuring range of the flow sensor is 0.1–5,000 ml/min.

Difference flow loggings were performed in two different campaigns in KFM01D /3/ and KFM08C /4/.

3.4 Boremap loggings

The drill cores of KFM01D /7/ and KFM08C /8/ were logged together with a simultaneous study of video images of the borehole wall. This is called Boremap logging.

In the core log, fractures parting the core are recorded. Fractures parting the core that have not been induced during the drilling or core handling are called broken fractures. To decide if a fracture actually was open or sealed in the rock volume (i.e. in situ), SKB has developed a confidence classification expressed at three levels, “possible”, “probable” and “certain”, based on the weathering and fit of the fracture surfaces /7/. However, there is a strong uncertainty associated with determining whether broken fractures were open or not before drilling /8/. For this reason, it was decided to treat all broken fractures as potentially open in situ in this present report.

In the Boremap logging, parts of the core that are crushed or lost are also recorded, as well as the spatial distribution of different rock types.

4 Execution

4.1 Theory

4.1.1 The formation factor

The theory applied for obtaining formation factors by electrical methods is described in /9/. The formation factor is the ratio between the diffusivity of the rock matrix to that of free pore water. If the species diffusing through the porous system is much smaller than the characteristic length of the pores and no interactions occur between the mineral surfaces and the species, the formation factor is only a geometrical factor that is defined by the transport porosity, the tortuosity and the constrictivity of the porous system:

$$F_f = \frac{D_e}{D_w} = \varepsilon_t \frac{\delta}{\tau^2} \qquad 4\text{-}1$$

where F_f (–) is the formation factor, D_e (m^2/s) is the effective diffusivity of the rock, D_w (m^2/s) is the diffusivity in the free pore water, ε_t (–) is the transport porosity, τ (–) is the tortuosity, and δ (–) is the constrictivity. When obtaining the formation factor with electrical methods, the Einstein relation between diffusivity and ionic mobility is used:

$$D = \frac{\mu RT}{zF} \qquad 4\text{-}2$$

where D (m^2/s) is the diffusivity, μ ($m^2/V \cdot s$) is the ionic mobility, z (–) the charge number and R (J/mol·K), T (K) and F (C/mol), are the gas constant, temperature, and Faraday constant, respectively. From the Einstein relation it is easy to show that the formation factor also is given by the ratio of the pore water resistivity to the resistivity of the saturated rock /10/:

$$F_f = \frac{\rho_w}{\rho_r} \qquad 4\text{-}3$$

where ρ_w (Ωm) is the pore water resistivity and ρ_r (Ωm) is the rock resistivity. The resistivity of the saturated rock can easily be obtained by standard geophysical methods.

At present it is not feasible to extract pore water from the rock matrix in situ. Therefore, it is assumed that the pore water is in equilibrium with the free water surrounding the rock, and measurements are performed on this free water. The validity of this assumption has to be discussed for every specific site.

In a new line of experiments, species in the pore water in drill core samples brought to the laboratory are leached. This has been done for a number of boreholes /e.g. 11/ and was also done in KFM01D. From the measured chloride content the EC of the pore water can be assessed. The assessed pore water EC was used as an integrated part when assessing the electrical conductivity profiles of the groundwater in KFM01D and KFM08C.

The resistivity is the reciprocal to electrical conductivity. Traditionally the EC (electrical conductivity) is used when measuring on water and resistivity is used when measuring on rock.

4.1.2 Surface conductivity

In intrusive igneous rock the mineral surfaces are normally negatively charged. As the negative charge often is greater than what can be balanced by cations specifically adsorbed on the mineral surfaces, an electrical double layer with an excess of mobile cations will form at the pore wall. If a potential gradient is placed over the rock, the excess cations in the electrical double layer will move. This process is called surface conduction and this additional conduction may have to be accounted for when obtaining the formation factor of rock saturated with a pore water of low

ionic strength. If the EC of the pore water is around 0.5 S/m or above, errors associated with surface conduction are deemed to be acceptable. This criterion is based on laboratory work by /12/ and /13/. The effect of the surface conduction on rock with formation factors below $1 \cdot 10^{-5}$ was not investigated in these works. In this report, surface conduction has not been accounted for, as in general only the groundwater in the upper 100 or 200 m of the boreholes has a low ionic strength and as more knowledge is needed on surface conduction before performing corrections.

4.1.3 Artefacts

Comparative studies have been performed on a large number of 1–2 cm long samples from Äspö /12/. Formation factors obtained with an electrical resistivity method using alternating current were compared to those obtained by a traditional through diffusion method, using Uranine as the tracer. The results show that formation factors obtained by the electrical resistivity measurements are a factor of about 2 times larger that those obtained by through diffusion measurements. A similar effect was found on granitic samples up to 12 cm long from Laxemar, using iodide in tracer experiments /14/. The deviation of a factor 2 between the methods may be explained by anion exclusion of the anionic tracers. Previously performed work suggests that the Nernst-Einstein equation between the diffusivity and electrical conductivity is generally applicable in granitic rock and that no artefacts give rise to major errors. It is uncertain, however, to what extent anion exclusion is related to the degree of compression of the porous system in situ due to the overburden.

4.1.4 Fractures in situ

In situ rock resistivity measurements are highly disturbed by free water in open fractures. The current sent out from the downhole tool in front of an open fracture will be propagated both in the porous system of the rock matrix and in the free water in the open fracture. Due to the low formation factor of the rock matrix, current may be preferentially propagated in a fracture intersecting the borehole if its aperture is on the order of 10^{-5} m or more.

There could be some confusion concerning the terminology of fractures. In order to avoid confusion, an organization sketch of different types of fractures is shown in Figure 4-1. The subgroups of fractures that interfere with the rock resistivity measurements are marked with grey.

The information concerning different types of fractures in situ is obtained from the interpretation of the Boremap logging and in the hydraulic flow logging. A fracture intersecting the borehole is most likely to part the drill core. In the core log, fractures that part the core are either broken or operational (drill-induced). Unbroken fractures, which do not part the core, are sealed or only partly open. Laboratory results suggest that sealed fractures generally have no major interference on rock resistivity measurements. The water-filled void in partly open fractures can be included in the porosity of the rock matrix.

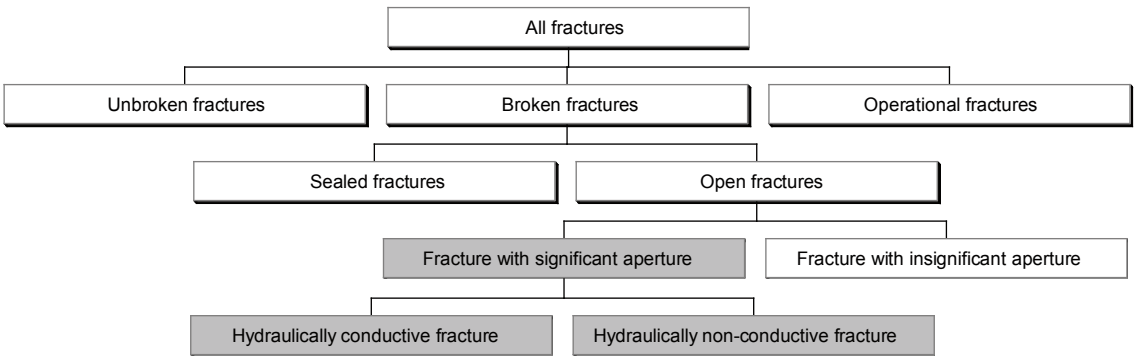

Figure 4-1. *Organization sketch of different types of fractures in situ.*

Broken fractures are either interpreted as open or sealed. Open fractures may have a significant or insignificant aperture. Insignificant aperture means an aperture so small that the amount of water held by the fracture is comparable with that held in the adjacent porous system. In this case the "adjacent porous system" is the porous system of the rock matrix the first few centimetres from the fracture.

If the fracture has a significant aperture, it holds enough water to interfere with the rock resistivity measurements. Fractures with a significant aperture may be hydraulically conductive or non-conductive, depending on how they are connected to the fracture network.

Due to uncertainties in the interpretation of the core logging, all broken fractures are assumed to potentially have a significant aperture in this present report.

4.1.5 Rock matrix and fractured rock formation factor

In this report the rock resistivity is used to obtain formation factors of the rock surrounding the borehole. The obtained formation factors may later be used in models for radionuclide transport in fractured crystalline rock. Different conceptual approaches may be used in the models. Therefore this report aims to deliver formation factors that are defined in two different ways. The first is the "rock matrix formation factor", denoted by F_f^{rm} (–). This formation factor is representative for the solid rock matrix, as the traditional formation factor. The other one is the "fractured rock formation factor", denoted by F_f^{fr} (–), which represents the diffusive properties of a larger rock mass, where fractures and voids holding stagnant water is included in the porous system of the rock matrix. Further information on the definition of the two formation factors could be found in /5/.

The rock matrix formation factor is obtained from rock matrix resistivity data. When obtaining the rock matrix resistivity log from the in situ measurements, all resistivity data that may have been affected by open fractures have to be sorted out. With present methods one cannot with certainty separate open fractures with a significant aperture from open fractures with an insignificant aperture in the interpretation of the core logging. It should be mentioned that there is an attempt to assess the fracture aperture in the interpretation of the core logging. However, this is done on a millimetre scale. Fractures may be significant even if they only have apertures some tens of micrometers.

By investigating the rock resistivity log at a fracture, one could draw conclusions concerning the fracture aperture. However, for formation factor logging by electrical methods this is not an independent method and cannot be used. Therefore, all broken fractures have to be considered as potentially open and all resistivities obtained close to a broken fracture detected in the core logging are sorted out. By examining the resistivity logs obtained by the Century 9072 tool, it has been found that resistivity values obtained within 0.5 m from a broken fracture generally should be sorted out. This distance includes a safety margin of 0.1–0.2 m.

The fractured rock formation factor is obtained from fractured rock resistivity data. When obtaining the fractured rock resistivity log from the in situ measurements, all resistivity data that may have been affected by free water in hydraulically conductive fractures, detected in the in situ flow logging, have to be sorted out. As mentioned above, with the Century 9072 tool, resistivity values obtained within 0.5 m from a hydraulically conductive fracture generally should be sorted out.

4.2 Rock resistivity measurements in situ

4.2.1 Rock resistivity log KFM01D

The rock resistivity of KFM01D was logged on the date 2006-03-08 (Sicada activity id 13104093) /1/. The in situ rock resistivity was obtained using the focused rock resistivity tool Century 9072. In situ rock resistivities, used in this present report, were obtained between the borehole lengths 92.5–798.3 m. In order to obtain an exact depth calibration, the track marks made in the borehole were used. According to /1/ an accurate depth calibration was obtained.

4.2.2 Rock matrix resistivity log KFM01D

All resistivity data obtained within 0.5 m from a broken fracture, detected in the core log, were sorted out from the in situ rock resistivity log. In the core log (Sicada activity id 13148042), a total of 662 broken fractures are recorded between 91.6–798.6 m. Four zones where the core has been crushed or lost were recorded. A total of 0.4 m of the core is crushed or lost. Broken fractures can potentially intersect the borehole in zones where the core is crushed or lost. Therefore, a broken fracture was assumed every decimetre in these zones. The locations of broken fractures in KFM01D are shown in Appendix A1. A total of 3,686 rock matrix resistivities were obtained between 92.5–798.3 m. 93% of the rock matrix resistivities were within the quantitative measuring range of the Century 9072 tool. The rock matrix resistivity log between 92.5–798.3 m is shown in Appendix A1.

Figure 4-2 shows the distribution of the rock matrix resistivities obtained between 92.5–798.3 m in KFM01D. The histogram ranges from 0–100,000 Ωm and is divided into sections of 5,000 Ωm.

4.2.3 Fractured rock resistivity log KFM01D

All resistivity data obtained within 0.5 m from a hydraulically conductive fracture, detected in the difference flow logging /3/, were sorted out from the in situ rock resistivity log. For the flow difference log, no correction in the reported borehole length was needed. A total of 34 hydraulically conductive fractures were detected in KFM01D between 81.6–790.9 m. The locations of hydraulically conductive fractures in KFM01D are shown in Appendix A1. A total of 6,652 fractured rock resistivities were obtained between 92.5–790.9 m. 92% of the fractured

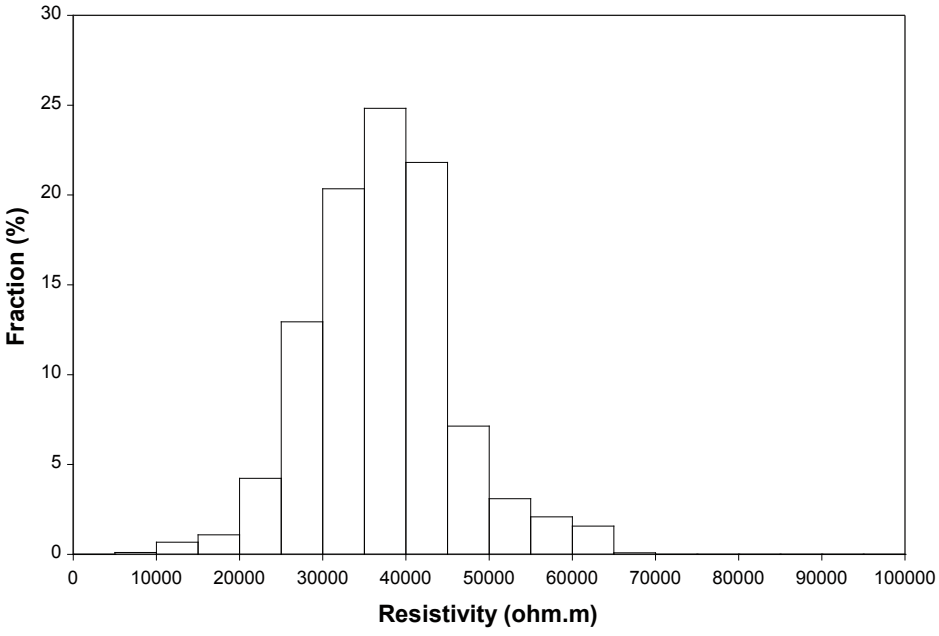

Figure 4-2. *Distribution of rock matrix resistivities in KFM01D.*

rock resistivities were within the quantitative measuring range of the Century 9072 tool. The fractured rock resistivity log between 92.5–790.9 m is shown in Appendix A1.

Figure 4-3 shows a histogram of the fractured rock resistivities obtained between 92.5–790.9 m in KFM01D. The histogram ranges from 0–100,000 Ωm and is divided into sections of 5,000 Ωm.

4.2.4 Rock resistivity KFM08C

The rock resistivity of KFM08C was logged on the date 2006-07-18 (Sicada activity id 13118290) /2/. The in situ rock resistivity was obtained using the focused Century 9072 tool. In situ rock resistivities, used in this present report, were obtained between the borehole lengths 13.1–949.5 m. In order to obtain an exact depth calibration, the track marks made in the borehole were used. According to /2/ an accurate depth calibration was obtained.

4.2.5 Rock matrix resistivity log KFM08C

All resistivity data obtained within 0.5 m from a broken fracture, detected in the core log, were sorted out from the in situ rock resistivity log. In the core log (Sicada activity id 13083977), a total of 1,129 broken fractures are recorded between 102.2–949.1 m. In addition three zones where the core is lost or crushed are recorded. A total of 1.2 m of the core is crushed or lost. Broken fractures can potentially intersect the borehole in zones where the core is crushed or lost. Therefore, a broken fracture was assumed every decimetre in these zones. The locations of broken fractures in KFM08C are shown in Appendix A2. A total of 4,050 rock matrix resistivities were obtained between 102.2–949.5 m. 96% of the rock matrix resistivities were within the quantitative measuring range of the Century 9072 tool. The rock matrix resistivity log between 102.2–949.5 m is shown in Appendix A2.

Figure 4-4 shows a histogram of the rock matrix resistivities obtained between 102.2–949.5 m in KFM08C. The histogram ranges from 0–100,000 Ωm and is divided into sections of 5,000 Ωm.

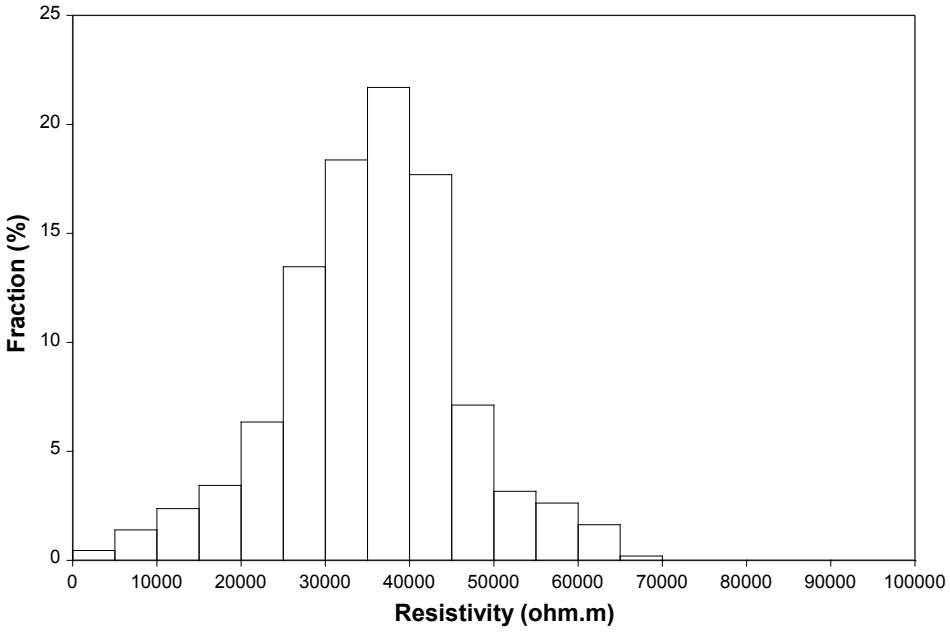

Figure 4-3. *Histogram of fractured rock resistivities in KFM01D.*

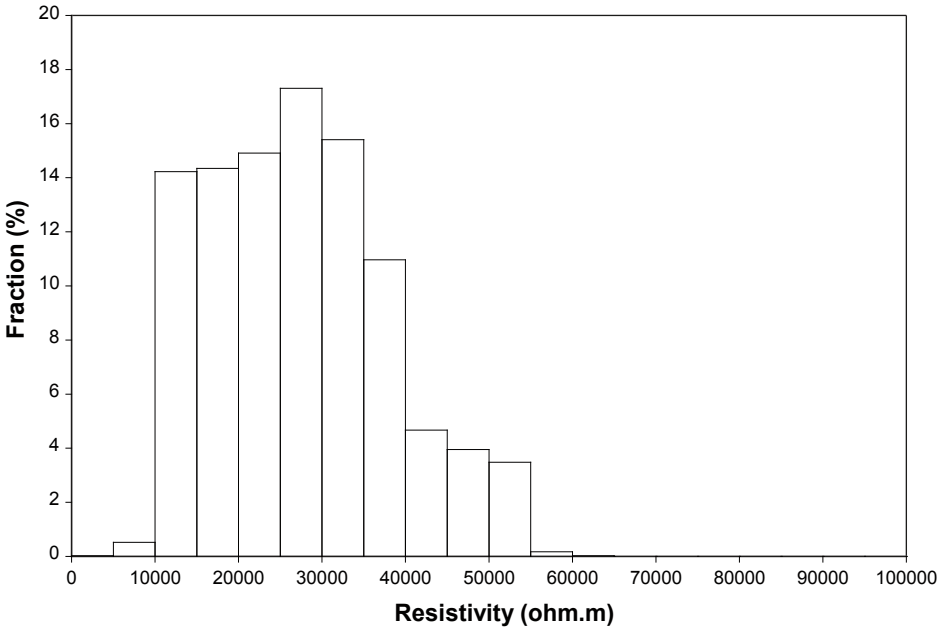

Figure 4-4. *Histogram of rock matrix resistivities in KFM08C.*

4.2.6 Fractured rock resistivity log KFM08C

All resistivity data obtained within 0.5 m from a hydraulically conductive fracture, detected in the difference flow logging /4/, were sorted out from the in situ rock resistivity log. For the difference flow log, no correction in the reported borehole length was needed. A total of 21 hydraulically conductive fractures were detected in KFM08C between 100.1–939.1 m. The locations of hydraulically conductive fractures in KFM08C are shown in Appendix A2. A total of 8,135 fractured rock resistivities were obtained between 100.1–939.1 m. 97% of the fractured rock resistivities were within the quantitative measuring range of the Century 9072 tool. The fractured rock resistivity log between 100.1–939.1 m is shown in Appendix A2.

Figure 4-5 shows a histogram of the fractured rock resistivities obtained between 100.1–939.1 m in KFM08C. The histogram ranges from 0–100,000 Ωm and is divided into sections of 5,000 Ωm.

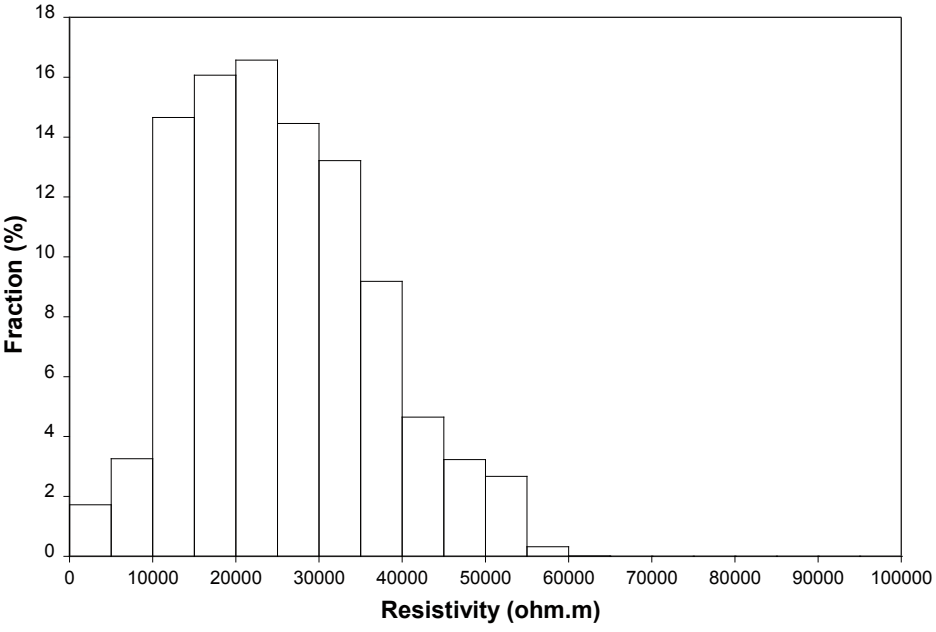

Figure 4-5. *Histogram of fractured rock resistivities in KFM08C.*

4.3 Groundwater EC measurements in situ

4.3.1 General comments

In background reports concerning the EC of the groundwater, some data have been corrected for temperature, so that they correspond to data at 25°C. Other EC data are uncorrected. Data that correspond to the temperature in situ should be used in in situ evaluations. Even though these corrections are small in comparison to the natural variation of the formation factor, measures have been taken to use data that correspond to the in situ temperature. Such data can in some cases be found in /15/.

Concerning borehole coordinates, unless specifically stated that the elevation is discussed, the borehole length is used. For elevation the unit m.a.s.l. (metres above sea level) is used.

4.3.2 Groundwater flow in KFM01D and KFM08C

When performing chemical characterisations of the groundwater at depth at the Forsmark site, the representativeness of the data may have to be considered. One way of doing this is to control the groundwater flow along the borehole, from one level to another. This has been done in previous reports concerning formation factor loggings in situ by electrical methods for the Laxemar subarea /e.g. 16/ but not for the Forsmark site.

When a borehole is drilled it functions as a hydraulic conductor, short-circuiting different hydraulic systems that the borehole intersects. The fact that groundwater flows from one depth to another in a borehole may affect the representativeness of the groundwater data obtained at a specific depth. At Forsmark, the hydraulic gradients over the boreholes are generally small and this results in relatively small flows of groundwater along the boreholes.

When measuring a fracture specific EC, by using the POSIVA difference flow meter or in the hydrochemical characterisations, a small section of the borehole is isolated by straddle packers. Water is then withdrawn from the fracture/fractures in the packed off borehole section and its EC is measured. However, if a large quantity of groundwater, representative for another depth, has flown along the short-circuiting borehole and into the fractures for weeks before the measurement, one can question the representativeness of the data obtained at that specific depth. It should be clarified that the measurements themselves may be accurate and still non-representative.

In hydraulic measurements in KFM01D /3/ and KFM08C /4/, 5-metres sections have been packed off and the flow into or out from (i.e. out from or into fractures intersecting the borehole) the boreholes in these sections has been measured by the POSIVA difference flow meter. This has been done when applying no drawdown (flow under natural gradient). The entire boreholes, except for the upper 100 metres or so, have been logged in this way by moving the tool step-wise. Based on these flow data, the flow along the boreholes when performing no pumping can be assessed. When doing this, a few assumptions are made.

1) If the flow in a section is below the measurement limit of the tool, no flow is accounted for.
2) It is assumed that there is no flow into or out from the lower end of the borehole.
3) The flow into and out from the borehole should be equal. In many cases no flow measurements are performed in the upper 100 m. This may be due to a casing or to other reasons. This is handled by lumping the in- and outflows, distributed over the section, into one in- or outflow term at ground surface.

Figure 4-6 shows the flow situation in KFM01D /3/. The red diamonds show the flow, where one could be found, into or out from the borehole in the packed off sections. A positive value represents a flow into the borehole and a negative value represents a flow out from the borehole. The grey line shows the flow along the borehole required to feed the in- and outflows. A positive value represents a flow down the borehole and a negative value represents a flow up the borehole.

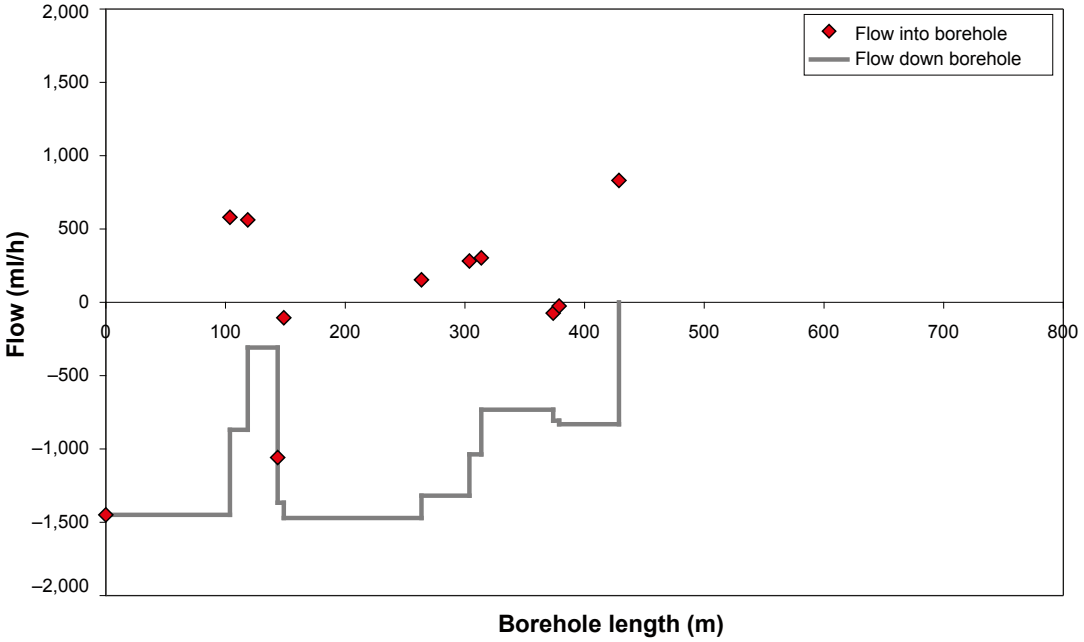

Figure 4-6. *Flow into/out from and down/up the borehole KFM01D.*

As can be seen in Figure 4-6 there is a small flow up the borehole from repository depth (i.e. 400–500 m). The borehole diameter is 76 mm and a flow of $4.5 \cdot 10^3$ ml/h along the borehole axis corresponds to a plug flow velocity of the borehole fluid of about 1 m/h. In KFM01D, the plug flow velocity at the borehole length 100 m should be about 0.3 m/h. The groundwater flow along the borehole was measured in situ at the borehole length 93 m. A small upward flow, around or below 1,000 ml/h, was detected when performing measurements without pumping /3/. Based on a mass balance approach, the flow up the borehole was assessed to around 1,500 ml/h in this report, which is in fair agreement with the measured flow.

Figure 4-7 shows the flow situation in KFM08C /4/. The legend is the same as in Figure 4-6.

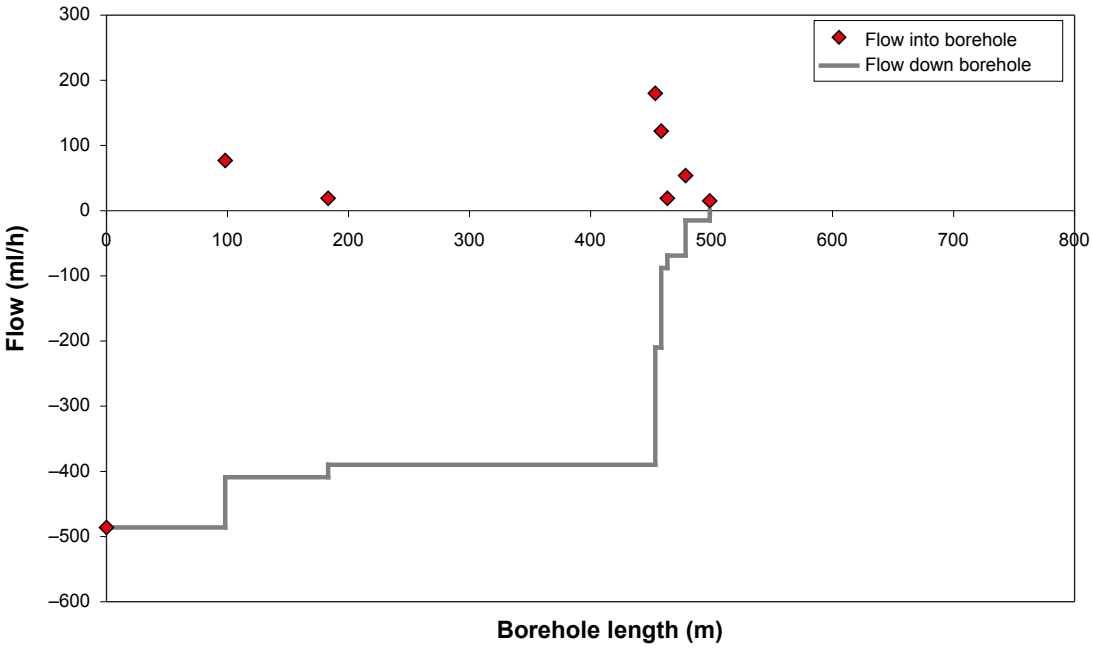

Figure 4-7. *Flow into/out of and down/up borehole KFM08C.*

As one can see by the grey line in Figure 4-7, there is a slight flow up the borehole from repository depth. The groundwater flow up the borehole was measured in situ at the borehole length 104 m to about 150 ml/h when performing no pumping /4/. Based on the mass balance approach, the flow up the borehole at this length was assessed to about 400 ml/h in this report, which is in fair agreement with the measured flow.

As there are so small flows along these boreholes, and as the flow is directed upwards, preventing non-saline water from the surface system to penetrate down the borehole, it is judged that all accurate groundwater EC data obtained at specific borehole lengths are also representative.

4.3.3 EC measurements in KFM01D

The EC of the borehole fluid in KFM01D was measured before and after performing extensive pumping on the dates 2006-05-23 to 2006-05-24 and 2006-05-31 to 2006-06-01, respectively /3/. The lines in Figure 4-8 represent the borehole fluid EC logs obtained before (blue) and after (green) performing extensive pumping. The fracture specific EC was measured on four locations on the dates 2006-05-30 to 2006-05-31 and the obtained fracture specific ECs are shown in Figure 4-8 as black crosses. The purple dots represent transient (time series) fracture specific ECs.

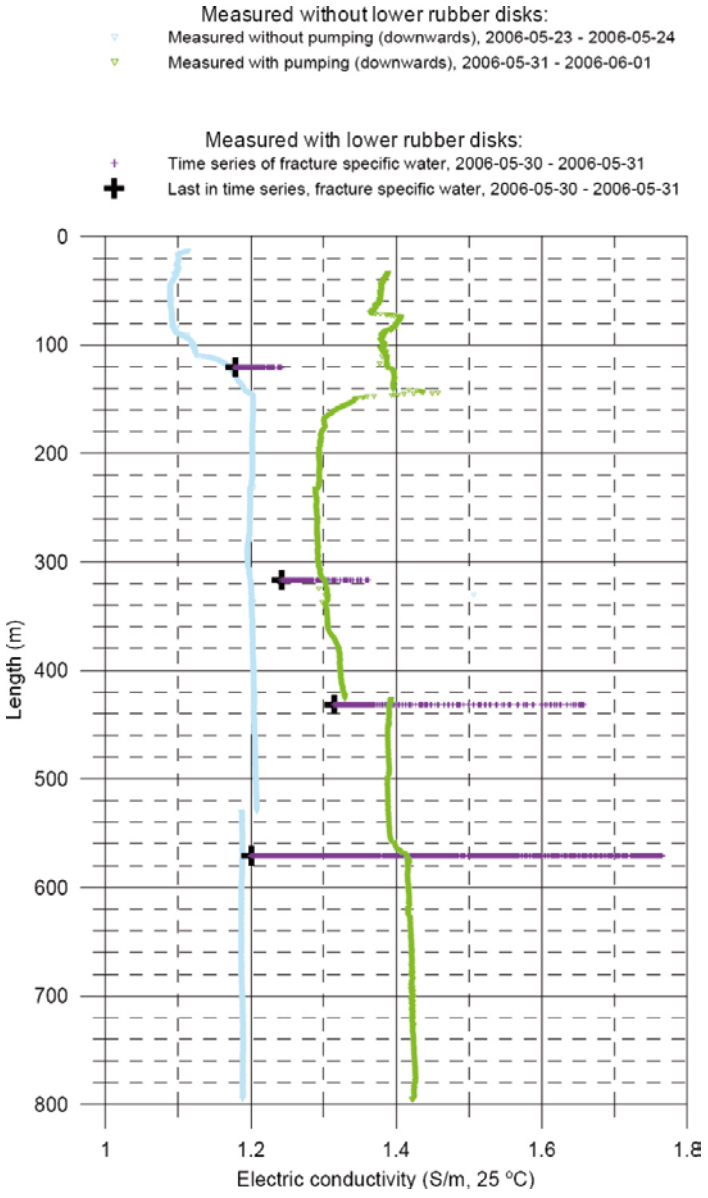

Figure 4-8. *EC logs in KFM01D. Image taken from /3/.*

As can be in Figure 4-8, the borehole fluid EC obtained prior to, and after performing extensive pumping does not deviate much. One can suspect that somewhat more saline groundwater has been pumped up the borehole from depth prior to the second measurement. According to /3/, there are no hydraulically conductive fractures below 571.2 m, at least not with a flow rate within the detection range of the tool. The fact that the borehole fluid in the lower part of the borehole (green line) has a higher EC than the fracture specific EC at 571.2 (black cross) tempts one to speculate that there indeed are hydraulically conductive fractures below 571.2 m, with more saline groundwater, but with such a low flow that they do not show on the flow log. However, the transient ECs for the fractures at 571.2 and 431.5 show peak values even higher than this, which may speak against making such speculations. It is noted that only low fractions of Uranine spiked flushing water was found in the hydrochemical characterisation at depth /6/. With these considerations, it is still assumed that the groundwater EC at 800 m corresponds to the highest borehole fluid EC shown by the green line in Figure 4-8. From the data in /3/ it is judged that the four fracture specific ECs obtained in KFM01D are representative from the groundwater at the corresponding depth. The data are shown in Table 4-1.

In addition to EC measurements with the Posiva flow log, the EC was also measured in the hydrogeochemical groundwater characterisations in KFM01D /6/ using the Chemmac equipment, between the borehole lengths 428.5 to 435.64 m (Sicada document ID 13125612) and 568 to 575.15 m (Sicada document ID 13125646). The hydrochemical characterisations were carried out between the dates 2006-06-07 and 2006-07-04, for the fracture at 431.5 m, and 2006-07-07 and 2006-08-01, for the fracture at 571.2 m. The reported ECs at 25°C are shown in Table 4-1.

In KFM01D two new sampling methods, SLT sampling and PSS sampling, were used to obtained fracture specific EC data. Four sections (see Table 4-1) were sampled with the SLT method between the dates 2006-08-03 and 2006-08-10 and one section was PSS sampled between the dates 2006-08-14 and 2006-08-22. Although these methods have not been generally used in the site investigations, and it may remain work to verify their accuracy, the delivered EC data are well in line with other EC data for KFM01D and therefore, it was decided to use the SLT and PSS data in this present report. As all data delivered in /6/, the SLT and PSS data are corrected to 25°C. In Table 4-1, the corresponding values at in situ temperature are shown. When obtaining these ECs, the same temperature correction as used for the Posiva difference

Table 4-1. Fracture specific ECs, KFM01D.

Measurment	Borehole section (m)	Location of fracture Borehole length (m)	Location of fracture Elevation (m.a.s.l.)	EC in situ (S/m)	EC 25°C (S/m)
Frac. Spec. EC	120.6–121.1	120.9	–96.0	0.77[a]	1.18[c]
SLT sampling	194.0–195.0	194.4	–155.6	0.69[b]	1.04[d]
SLT sampling	263.8–264.8	264.3	–211.4	0.75[b]	1.10[d]
PSS samling	314.5–319.5	316.9	–252.8	0.81[b]	1.18[d]
Frac. Spec. EC	316.66–317.16	319.9	–255.6	0.85[a]	1.24[c]
SLT sampling	354.9–355.9	355.2	–282.7	0.80[b]	1.16[d]
SLT sampling	369.0–370.0	369.5	–293.8	0.84[b]	1.23[d]
Frac. Spec. EC	431.3–431.8	431.5	–341.5	0.92[a]	1.31[c]
Hydrochem char	428.5–435.64	431.5	–341.5	0.98[b]	1.4[a]
Frac. Spec. EC	570.8–571.3	571.2	–446.6	0.87[a]	1.20[c]
Hydrochem char	568–575.14	571.2	–446.6	1.3[b]	1.8[a]
Borehole fluid	800.0	800.0	–612.3	1.07[a]	1.43[a]

[a] Data from Sicada.

[b] Data corrected to in situ temperature by using correction factor from Sicada document ID 13115486.

[c] Data from /3/.

[d] Data from /6/.

flow log measurements /15/ at the corresponding borehole length was applied. In addition to measuring the fracture specific EC at certain depths, an attempt was made to obtain the chloride concentration of the matrix fluid (pore water) of samples taken from the drill core of KFM01D. The method is described in /e.g. 11/. Table 4-2 shows the obtained chloride concentrations and references to the Sicada document where the data can be found.

In order to convert chloride concentrations to EC data, information from the hydrochemical characterisation at the Forsmark site was used. Data from measurements with the Chemmac equipment in borehole KFM01D, KFM03A, KFM04A, KFM06A, KFM08A, and KFM09A were used. In these measurements, both the chloride concentration and EC (at 25°C) are measured for the same groundwater. Figure 4-9 (upper) shows the EC (at 25°C) vs. Cl^- concentration for a number of Chemmac measurements. The numerical values of the data points, and references to the measurements, can be found in Appendix C.

For reference, a similar plot of the Cl^- concentration vs. EC (at 25°C) is taken from /6/ and shown in Figure 4-9 (lower). In Figure 4-9 (lower), EC data obtained in KFM01D are shown as purple squares and dark blue diamonds represent EC data obtained with different techniques in the Forsmark area. The motive for not basing the calibration of the EC (at 25°C) vs. Cl^- concentration on the fitting made in /6/ is simply that /6/ was published after data from this present report were delivered to Sicada. Another motive is that other equipments than the Chemmac equipment have been used to obtain many data points. In any case, as can be seen the deviation between the two fittings is very small.

The linear fitting in Figure 4-9 (upper) is described by the equation:

$$EC\ (S/m) = 0.37 + 0.22 \cdot Cl^-\ (g/kg\ H_2O) \qquad 4\text{-}4$$

By using this equation, the EC at 25°C was assessed for the matrix fluid. The data are shown in Table 4-2. To convert these data to in situ ECs, the temperature correction factors used for the Posiva difference log (Sicada document ID 13115486) were used, at corresponding depths.

Table 4-2. Matrix fluid ECs in KFM01D.

Sicada Activity ID	Borehole length (m)	Elevation (m.a.s.l.)	Chloride concentration (mg Cl^-/kg)	EC at 25°C (S/m)	In situ EC[a] (S/m)
13150811	140.7	–112.1	2,846	1.00	0.66
13150812	191.7	–153.7	2,251	0.87	0.58
13150813	255.1	–204.5	4,008	1.25	0.84
13150814	299.1	–239.3	2,736	0.97	0.66
13150815	352.1	–280.5	3,334	1.10	0.76
13150816	393.7	–312.5	2,933	1.02	0.71
13150817	462.8	–365.5	2,406	0.90	0.63
13150818	500.1	–393.5	2,634	0.95	0.67
13150819	544.2	–426.5	2,976	1.02	0.73
13150820	600.3	–468.1	2,356	0.89	0.65
13150821	643.1	–499.5	2,997	1.03	0.75
13150824	700.3	–541.0	3,038	1.04	0.77
13150825	747.3	–574.8	4,204	1.29	0.96
13150827	790.6	–605.6	5,743	1.63	1.23

[a]Data corrected to in situ temperature by using correction factor from Sicada document ID 13115486.

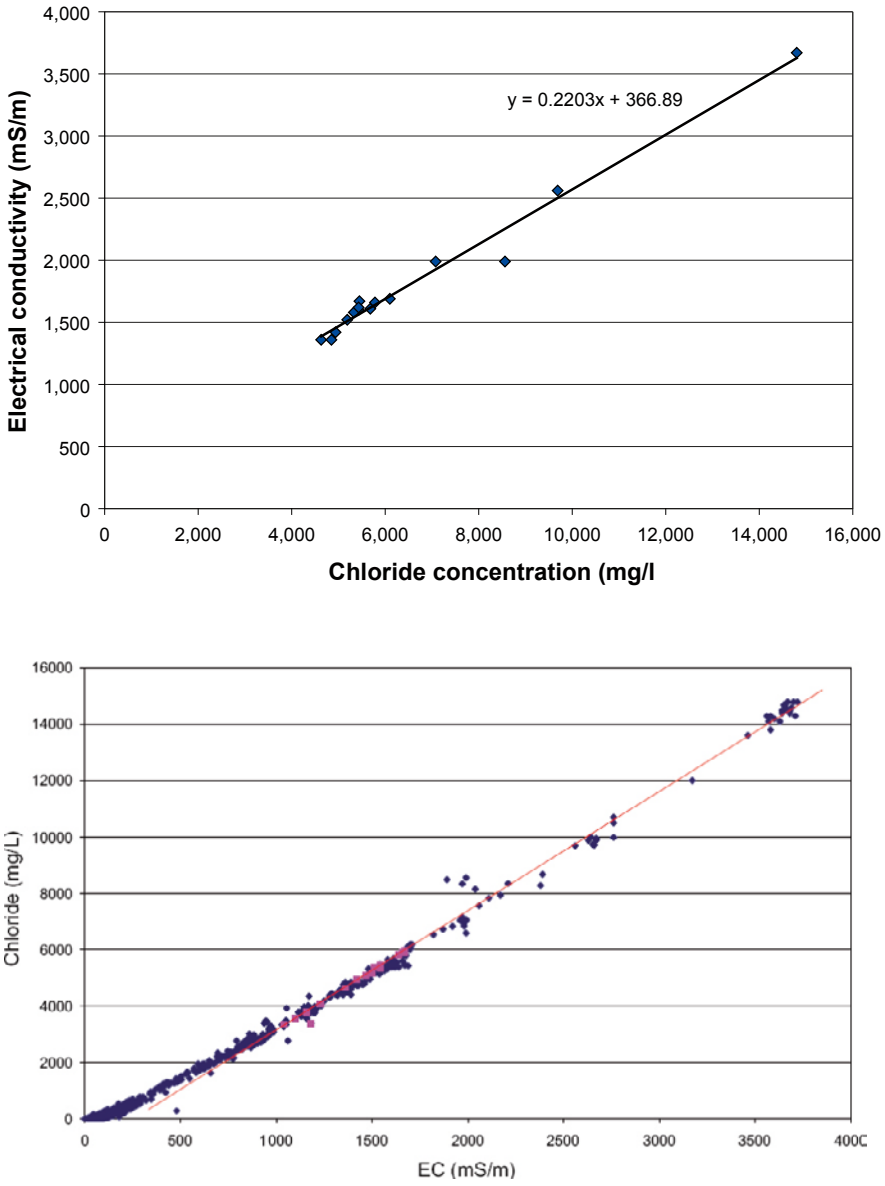

Figure 4-9. *Chloride concentration vs. electrical conductivity in Forsmark. Upper plot based on Chemmac measurements. Lower plot taken from /6/.*

4.3.4 EC measurements in KFM08C

The EC of the borehole fluid in KFM08C was measured before and after performing extensive pumping on the dates 2006-06-05 to 2006-06-06 and 2006-06-18, respectively /4/. The lines in Figure 4-10 represent the borehole fluid EC logs obtained before (blue) and after (green) performing extensive pumping. The fracture specific EC was measured on three locations on the dates 2006-06-17 to 2006-06-18 and the obtained fracture specific ECs are shown in Figure 4-10 as black crosses. The purple dots represent transient (time series) fracture specific ECs.

As can be in Figure 4-10, the borehole fluid EC obtained prior to and after performing extensive pumping does not deviate much. It is unusual though that the borehole fluid EC is lower after the pumping than before. Furthermore, it is difficult to suggest any explanation (except for experimental errors etc.) for this behaviour. As can be seen from Figure 4-10, the fracture specific ECs (black crosses) are within the range of the two borehole fluid EC logs. As shown in Figure 4-7, there is no indication of a flow of non-saline groundwater from the surface system, penetrating down the borehole. Furthermore, from the transient fracture specific EC

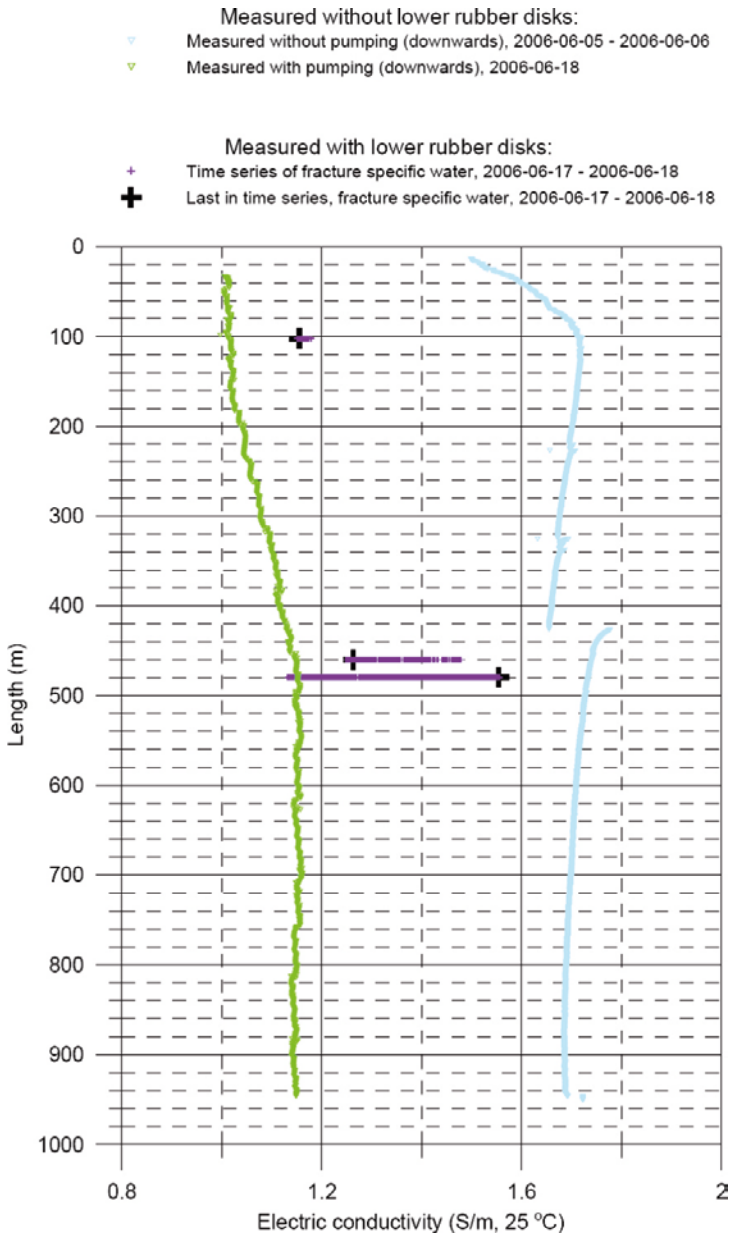

Figure 4-10. *EC logs in KFM08C. Image taken from /4/.*

logs /4/ there are no indications of major problems in the measurements, even though one could speculate that the ECs value obtained at 479.7 m could have been somewhat higher if extending the measurement period. It is judged that the obtained fracture specific ECs are sufficiently representative for the purpose of this report. The data are shown in Table 4-3.

In addition to measuring the fracture specific EC at certain depths, an attempt was made to obtain the chloride concentration of the matrix fluid (pore water) of samples taken from the drill core of KFM08C. Table 4-4 shows the obtained chloride concentrations and references to the Sicada document where the data can be found.

By using Equation 4-4, the EC at 25°C was assessed for the matrix fluid. The data are shown in Table 4-4. To convert these data to in situ ECs, the temperature correction factors used for the Posiva difference log (Sicada document ID 13116252) were used, at corresponding depths. EC data at in situ temperature are shown in Table 4-4.

Table 4-3. Fracture specific ECs, KFM08C.

Measurment	Borehole section (m)	Location of fracture Borehole length (m)	Location of fracture Elevation (m.a.s.l.)	EC in situ (S/m)	EC 25°C (S/m)
Frac. Spec. EC	102.05	102.55	102.4	0.76[a]	1.16[b]
Frac. Spec. EC	460.23	460.73	460.5	0.89[a]	1.26[b]
Frac. Spec. EC	479.74	480.24	480.0	1.10[a]	1.55[b]

[a] Data from Sicada.

[b] Data from /4/.

Table 4-4. Matrix fluid ECs in KFM08C.

Sicada Activity id	Borehole length (m)	Elevation m.a.s.l.)	Chloride concentration (mg Cl^-/kg)	EC at 25°C (S/m)	In situ EC[a] (S/m)
13150822	154.7	–131.2	2,177	0.85	0.56
13150823	254.9	–215.9	2,111	0.83	0.56
13150826	353.9	–298.6	3,092	1.05	0.72
13150828	455.7	–383.0	4,464	1.35	0.96
13150829	553.2	–463.2	6,241	1.74	1.25
13150830	600.9	–502.1	4,249	1.30	0.95
13150831	751.45	–623.3	14,686	3.60	2.73
13150832	839.7	–693.3	10,128	2.60	2.01
13150833	917.2	–754.4	11,032	2.80	2.22
13150834	938.3	–770.8	10,627	2.71	2.15

[a]Data corrected to in situ temperature by using correction factor from Sicada document ID 13116252.

4.3.5 EC profiles in KFM01D and KFM08C

The in situ EC data shown in Tables 4-1 to 4-4 are plotted vs. elevation for the boreholes KFM01D and KFM08C in Figure 4-11. Triangles represent EC data obtained on freely flowing groundwater and dots represent matrix fluid ECs.

From these data, EC profiles representative for the groundwater surrounding the two boreholes were assessed. It is acknowledged that there is a degree of subjectivity in assessing the EC profiles. For example, the EC data point for KFM08C at –623 m above sea level was considered to be an outlier. Based on the data it was decided that each borehole should be fitted by two straight lines, one above and one below –572 m above sea level. The assessed EC profile for KFM01D is shown by the red lines in Figure 4-11, and the assessed EC profile for KFM08D is shown by the blue lines.

When converting the elevation to borehole length, the equations for the two fittings for KFM01D become:

KFM01D: borehole length 120–743 m,

$$\text{EC (S/m)} = 2.21 \cdot 10^{-4} \times \text{borehole length (m)} + 0.729 \qquad 4\text{-}5$$

KFM01D: borehole length 743–800 m,

$$\text{EC (S/m)} = 4.79 \cdot 10^{-3} \times \text{borehole length (m)} - 2.66 \qquad 4\text{-}6$$

It is recommended not to extrapolate Equation 4-5 to shallower borehole lengths than 120 m.

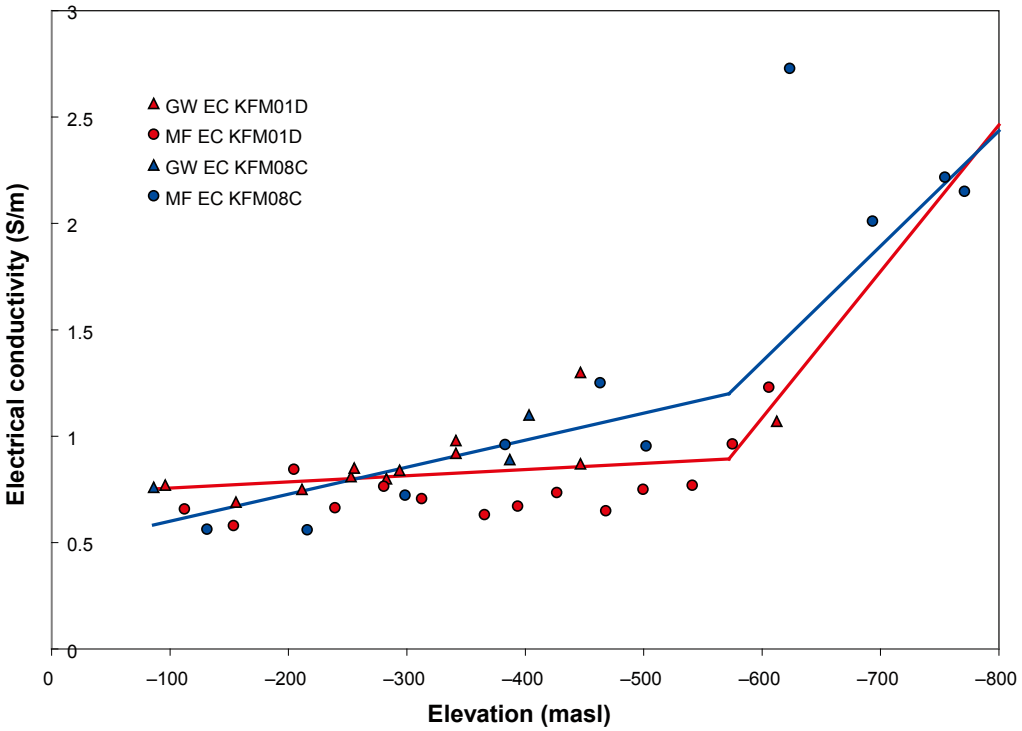

Figure 4-11. *Groundwater and pore water EC at in situ temperature in KFM01D and KFM08C.*

When converting the elevation to borehole length of KFM08C, the equations for the two fittings become:

KFM08C: borehole length 86–688 m,
EC (S/m) = $1.06 \cdot 10^{-3}$ × borehole length (m) + 0.475 4-7

KFM08C: borehole length 688–1,000 m,
EC (S/m) = $4.29 \cdot 10^{-3}$ × borehole length (m) –1.75 4-8

It is recommended not to extrapolate Equation 4-7 to shallower borehole lengths than 86 m.

4.3.6 Electrical conductivity of the pore water

The assessed EC profiles for the groundwater in the rock mass surrounding KFM01D and KFM08C, shown in Figure 4-11, are to a large extent based upon measurements on the pore water (matrix fluid). Therefore, it is judged that the profiles are also representative for the pore water.

4.4 Formation factor measurements in the laboratory

The formation factor was measured in the laboratory on a single drill core sample from KFM08C /17/. The method for doing this is described in /17/. The sample measured on was taken between the borehole lengths 830.64–830.67 m. The obtained formation factor was $2.09 \cdot 10^{-4}$.

4.5 Nonconformities

The work was carried out in accordance with the Activity Plan and the Method Description. Except for the fact that the formation factors of KFM08C, and not KFM06C, were assessed this was done without nonconformities. The decision to change KFM06A for KFM08C was made by SKB.

The limited quantitative measuring range of the in situ rock resistivity tool may give rise to overestimations of formation factors in the lower formation factor range.

5 Results

5.1 General

Original data from the reported activity are stored in the primary database Sicada. Data are traceable in Sicada by the Activity Plan number (AP PF 400-06-099). Only data in databases are accepted for further interpretation and modelling. The data presented in this report are regarded as copies of the original data. Data in the databases may be revised, if needed. However, such revision of the database will not necessarily result in a revision of this report, although the normal procedure is that major data revisions entail a revision of P-reports. Minor data revisions are normally presented as supplements, available at www.skb.se.

5.2 In situ rock matrix formation factor

The in situ formation factors obtained in KFM01D and KFM08C were treated statistically. By using the normal-score method, as described in /18/, to determine the likelihood that a set of data is normally distributed, the mean value and standard deviation of the logarithm ($\log_{10}$) of the formation factors could be determined. Figure 5-1 shows the distributions of the rock matrix formation factors obtained in situ between 120.0–798.3 m in KFM01D and between 102.2–949.5 m in KFM08A.

The rock matrix formation factors for KFM01D and KFM08C are relatively well log-normally distributed with a small variance. The number of data points, mean values and standard deviations of the distributions in Figure 5-1 are shown in Table 5-1 and Table 5-2 for KFM01D and KFM08C, respectively. The in situ rock matrix formation factor logs of KFM01D and KFM08C are shown in Appendix B1 and B2, respectively.

5.3 In situ fractured rock formation factor

Figure 5-2 shows the distributions of the fractured rock formation factors obtained in situ between 120.0–790.9 m in KFM01D and between 100.1–939.1 m in KFM08C.

The distributions strongly resemble those in Figure 5-1, except for a deviation in the upper formation factor region. Here, some of the obtained formation factors are affected by free water in hydraulically non-conductive fractures. The number of data points, mean values and standard deviations of the distributions in Figure 5-2 are shown in Table 5-1 and Table 5-2 for KFM01D and KFM08C, respectively. The in situ fractured rock formation factor logs of KFM01D and KFM08C are shown in Appendix B1 and B2, respectively.

5.4 Comparison of formation factors of KFM01D

Table 5-1 presents mean values and standard deviations of the log-normal distributions shown in Figures 5-1 and 5-2 for KFM01D. In addition, the number of data points obtained and the arithmetic mean values for the different formation factors are shown.

As seen in Table 5-1, the fractured rock formation factors are, on average, only slightly larger than the rock matrix formation factors. This is explained by the fact that much of the rock surrounding KFM01D is very sparsely fractured.

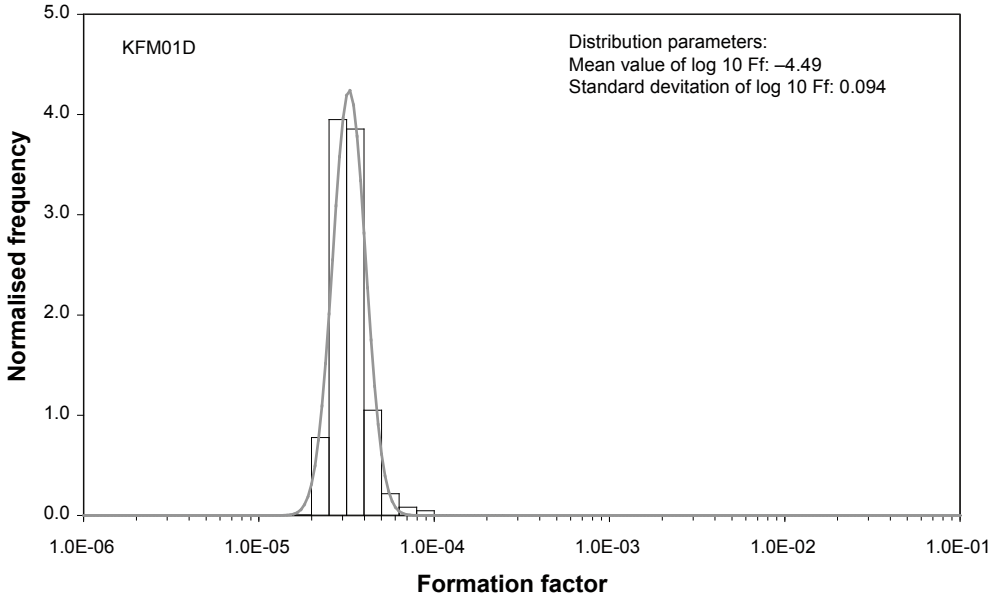

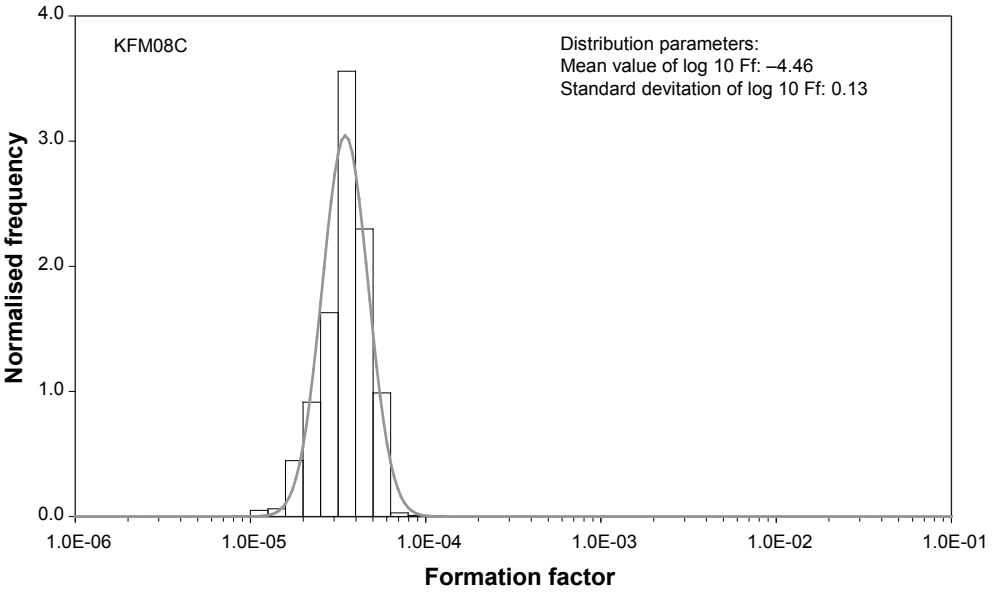

Figure 5-1. *Distributions of in situ rock matrix formation factors in KFM01D and KFM08C.*

Table 5-1. Distribution parameters and arithmetic mean value of the formation factor, KFM01D.

Formation factor	Number of data points	Mean $\log_{10}(F_f)$	Standard deviation $\log_{10}(F_f)$	Arithmetic mean F_f
In situ Rock matrix F_f	3,636	–4.49	0.094	$3.37 \cdot 10^{-5}$
In situ Fractured rock F_f	6,388	–4.45	0.15	$4.01 \cdot 10^{-5}$

Table 5-2. Distribution parameters and arithmetic mean value of the formation factor, KFM08C.

Formation factor	Number of data points	Mean $\log_{10}(F_f)$	Standard deviation $\log_{10}(F_f)$	Arithmetic mean F_f
In situ Rock matrix F_f	4,050	–4.46	0.13	$3.64 \cdot 10^{-5}$
In situ Fractured rock F_f	8,135	–4.39	0.20	$4.97 \cdot 10^{-5}$

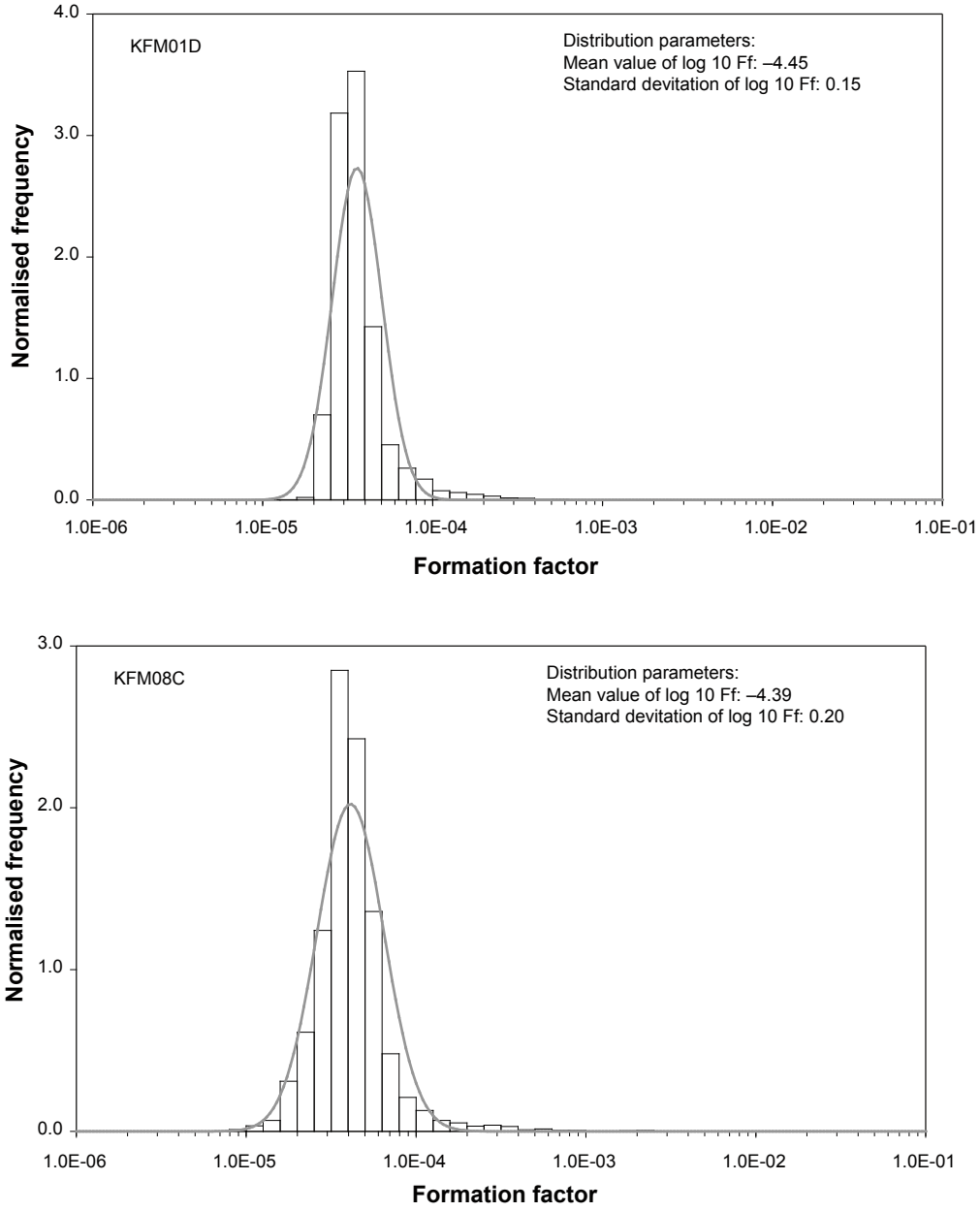

Figure 5-2. *Distributions of in situ fractured rock formation factors in KFM01D and KFM08C.*

5.5 Comparison of formation factors of KFM08C

Table 5-2 presents mean values and standard deviations of the log-normal distributions shown in Figures 5-1 and 5-2 for KFM08C. In addition, the number of data points obtained and the arithmetic mean values for the different formation factors are shown.

As seen in Table 5-2, the fractured rock formation factors are, on average, not that much larger than the rock matrix formation factors. This is explained by the fact that much of the rock surrounding KFM08C is sparsely fractured.

The rock matrix formation factors obtained in situ can be compared with the formation factor value $2.09 \cdot 10^{-4}$ obtained on a single drill core sample of KFM08C at the borehole length 830.66 m. However, by examining the core log /8/, one can see that the drill core sample consists of altered rock taken from a very fractured borehole section. Therefore, the increased value obtained in the laboratory may be expected.

6 Summary and discussions

The formation factors obtained in KFM01D and KFM08C range from $8.4 \cdot 10^{-6}$ to $2.2 \cdot 10^{-3}$. The formation factors appear to be fairly well distributed according to the log-normal distribution, even though there are some deviations in the upper formation factor range for the fractured rock formation factor distributions. The obtained in situ distributions have mean values for $\log_{10}(F_f)$ between –4.49 and –4.39 and standard deviations between 0.094 and 0.20. The arithmetic mean values for the boreholes range between $3.37 \cdot 10^{-5}$ and $4.97 \cdot 10^{-5}$. All in all, the variability of the formation factor in these boreholes is small.

The fractured rock formation factors were on average only slightly larger than the rock matrix formation factors. This indicates that the retention capacity for non-sorbing species due to open, but hydraulically non-conductive, fractures on average is less significant in the rock that generally surrounds these boreholes. However, these measurements do not necessarily give accurate information concerning the retention capacity of the rock directly adjacent to flowpaths. Formation factors in rock adjacent to flowpaths can very well be generally larger than those given in this report, but not likely smaller.

Judging from the obtained formation factor histograms, only a fraction (< 10%) of the obtained in situ rock resistivities may have been affected by limitations of the in situ rock resistivity tool.

References

/1/ **Nielsen U T, Ringgaard J, 2006.** Geophysical borehole logging in borehole KFM01D. Forsmark site investigation. SKB P-06-168, Svensk Kärnbränslehantering AB.

/2/ **Nielsen U T, Ringgaard J, 2007.** Geophysical borehole logging in boreholes KFM08C, KFM10A, HFM30, HFM31, HFM33, HFM34, HFM35 and HFM38. Forsmark site investigation. SKB P-07-05, Svensk Kärnbränslehantering AB.

/3/ **Väisäsvaara J, Leppänen H, Pekkanen J, 2006.** Difference flow logging in borehole KFM01D. Forsmark site investigation. SKB P-06-161, Svensk Kärnbränslehantering AB.

/4/ **Väisäsvaara J, Leppänen H, Pekkanen J, Pöllänen J, 2006.** Difference flow logging in borehole KFM08C. Forsmark site investigation. SKB P-06-189, Svensk Kärnbränslehantering AB.

/5/ **Löfgren M, Neretnieks I, 2005.** Formation factor logging in situ and in the laboratory by electrical methods in KSH01A and KSH02: Measurements and evaluation of methodology. Oskarshamn site investigation. SKB P-05-27, Svensk Kärnbränslehantering AB.

/6/ **Nilsson K, Bergelin A, Lindquist A, Nilsson A C, 2006.** Hydrochemical characterisation in borehole KFM01D. Results from seven investigated borehole sections: 194.0–195.0 m, 263.8–264.8 m, 314.5–319.5 m, 354.9–355.9 m, 369.0–370.0 m, 428.5–435.6 m, 568.0–575.1 m. Forsmark site investigation. SKB P-06-227, Svensk Kärnbränslehantering AB.

/7/ **Petersson J, Skogsmo G, von Dalwigk I, Wängnerud A, Berglund J, 2006.** Boremap mapping of telescopic drilled borehole KFM01D. Forsmark site investigation. SKB P-06-132, Svensk Kärnbränslehantering AB.

/8/ **Petersson J, Wängnerud A, von Dalwigk I, Berglund J, Andersson U B, 2006.** Boremap mapping of telescopic drilled borehole KFM08C. Forsmark site investigation. SKB P-06-203, Svensk Kärnbränslehantering AB.

/9/ **Löfgren M, Neretnieks I, 2002.** Formation factor logging in situ by electrical methods. Background and methodology. SKB TR-02-27, Svensk Kärnbränslehantering AB.

/10/ **Löfgren M, 2001.** Formation factor logging in igneous rock by electrical methods. Licentiate thesis at the Royal Institute of Technology, Stockholm, Sweden. ISBN 91-7283-207-x.

/11/ **Waber H N, Smellie J A T, 2005.** Borehole KFM06A: Characterisation of pore water. Part 1: Diffusion experiments. Forsmark site investigation. SKB P-05-196, Svensk Kärnbränslehantering AB.

/12/ **Ohlsson Y, 2000.** Studies of Ionic Diffusion in Crystalline Rock. Doctoral thesis at the Royal Institute of Technology, Stockholm, Sweden. ISBN 91-7283-025-5.

/13/ **Löfgren M, 2004.** Diffusive properties of granitic rock as measured by in situ electrical methods. Doctoral thesis at the Royal Institute of Technology, Stockholm, Sweden. ISBN 91-7283-935-X.

/14/ **Löfgren M, Neretnieks I, 2006.** Through-electromigration: A new method of investigating pore connectivity and obtaining formation factors. Journal of Contaminant Hydrology, Vol. 87 (3–4), pp. 237–252.

/15/ **SICADA, 2007.** Site Characterisation Data Base, Svensk Kärnbränslehantering AB.

/16/ **Löfgren M, Neretnieks I, 2005.** Formation factor logging in situ by electrical methods in KLX03 and KLX04. Oskarshamn site investigation. SKB P-05-105, Svensk Kärnbränslehantering AB.

/17/ **Thunehed H, 2007.** Complementary resistivity measurements on samples from KFM01A, KFM02A, KFM06A, KFM08A, KFM08C and KFM09A. Forsmark site investigation. SKB P-07-137, Svensk Kärnbränslehantering AB.

/18/ **Johnson RA, 1994.** Miller and Freund's probability & statistics for engineers, 5ed. Prentice-Hall Inc., ISBN 0-13-721408-1.

Appendix A1: In situ rock resistivities and fractures KFM01D

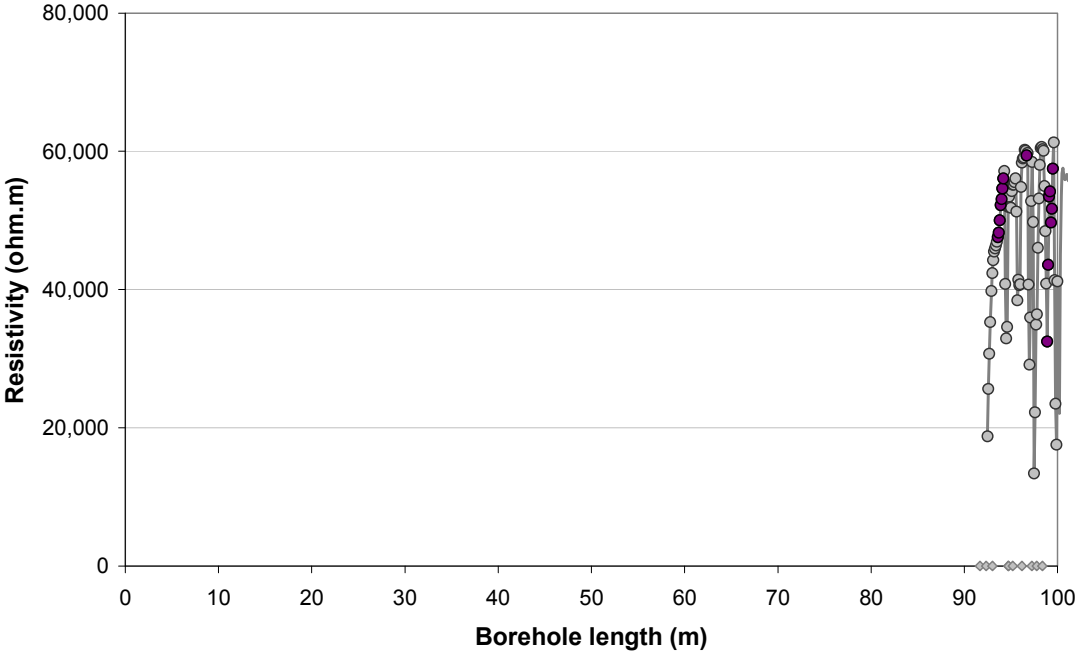

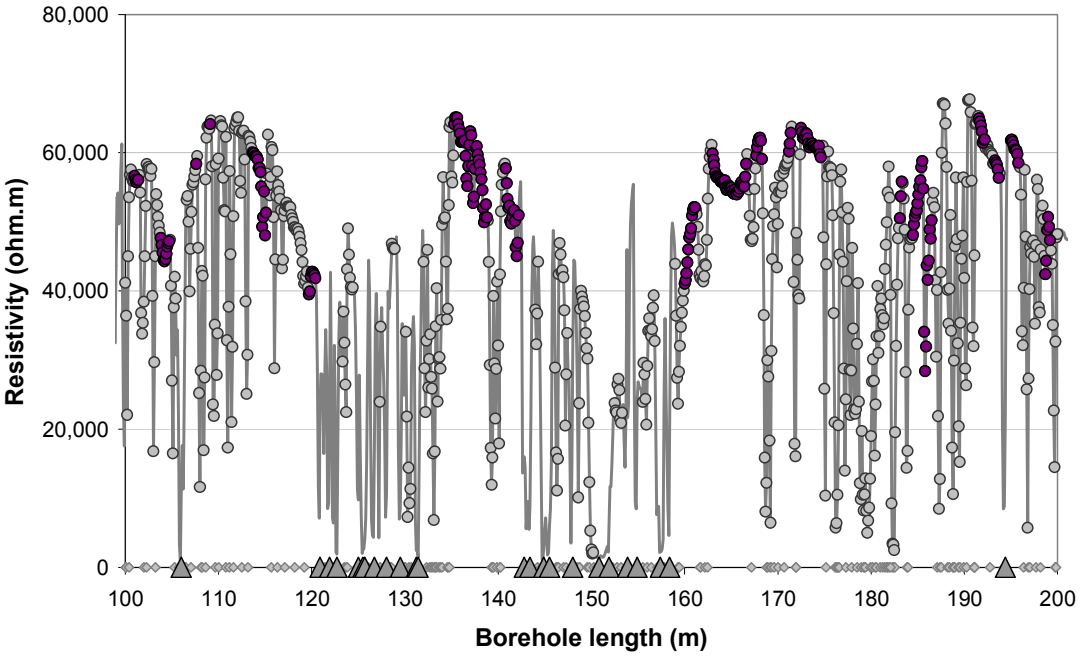

Rock resistivity
Fractured rock resistivity
Rock matrix resistivity
Location of broken fracture parting the drill core
Location of hydraulically conductive fracture detected in the difference flow logging

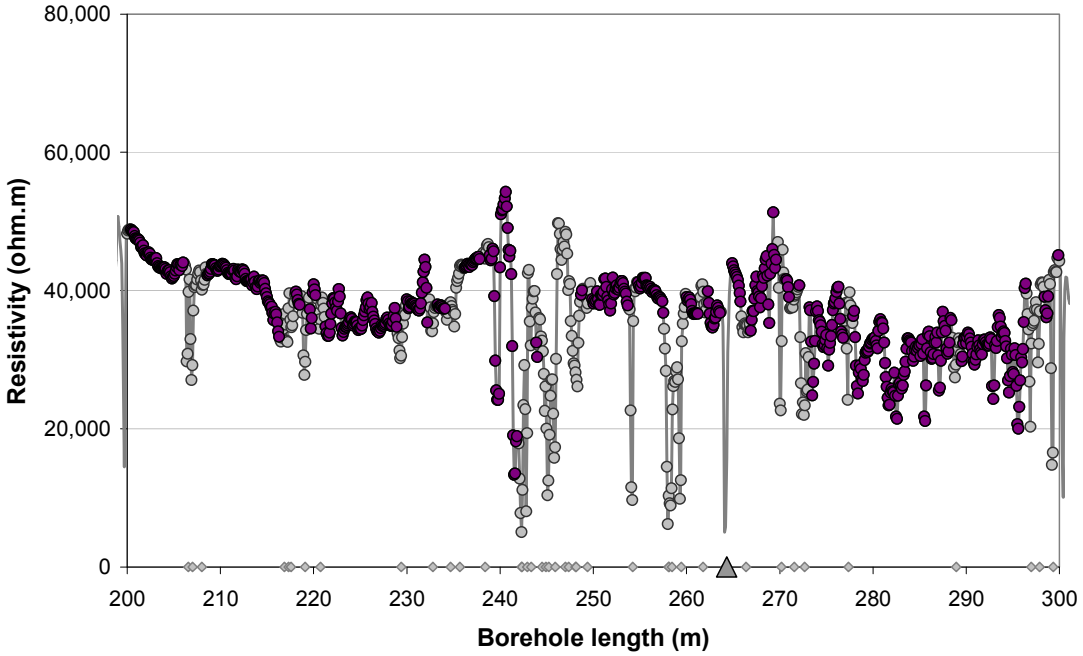

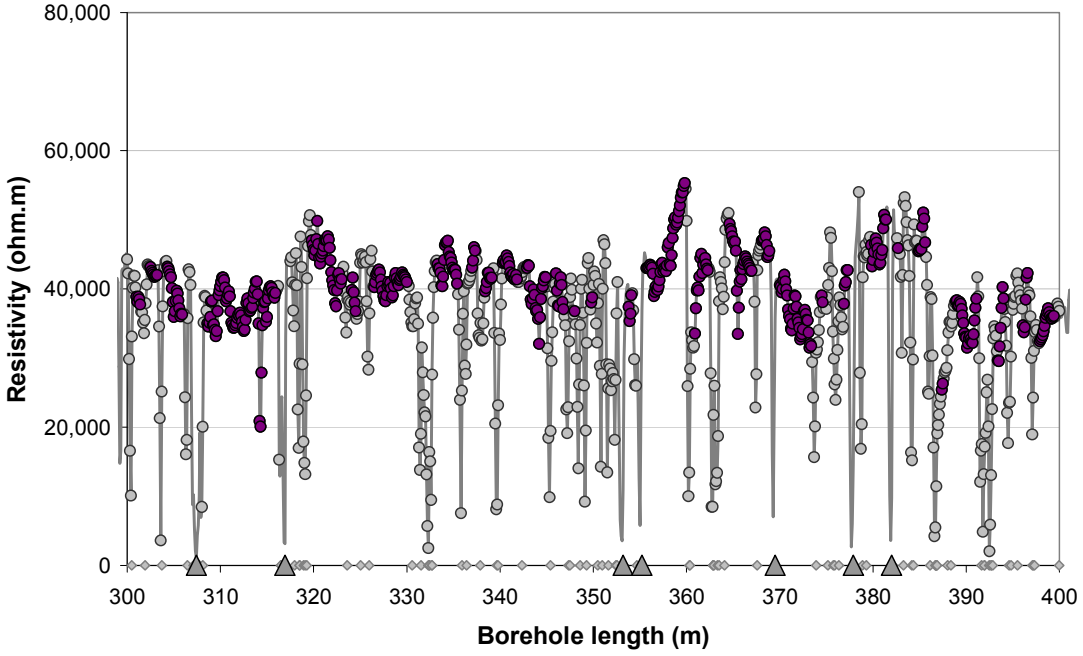

Rock resistivity
Fractured rock resistivity
Rock matrix resistivity
Location of broken fracture parting the drill core
Location of hydraulically conductive fracture detected in the difference flow logging

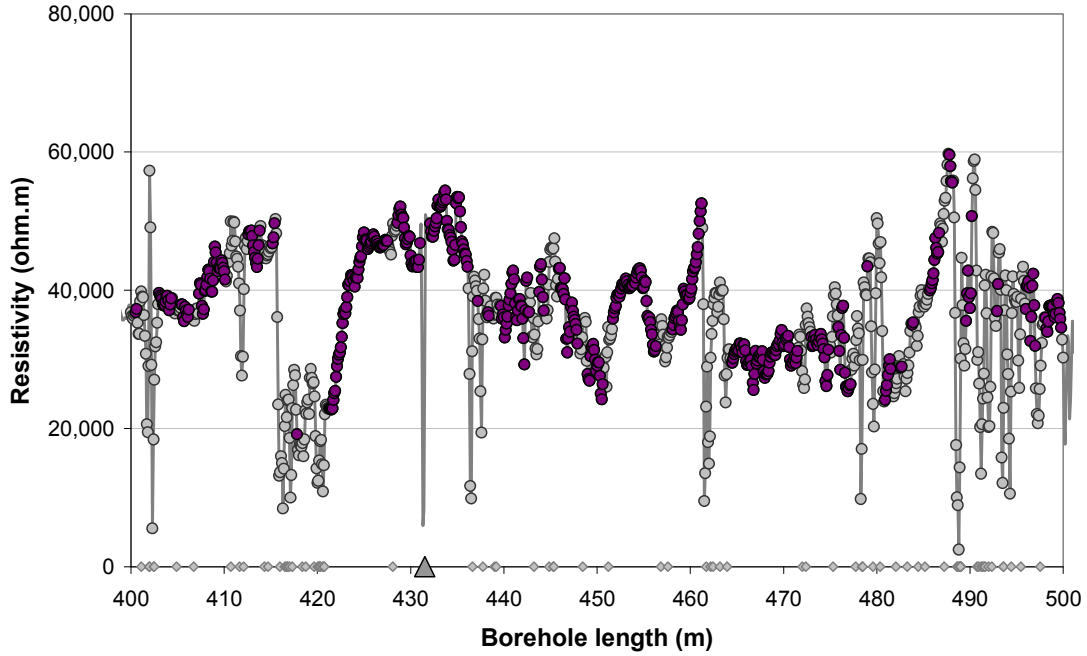

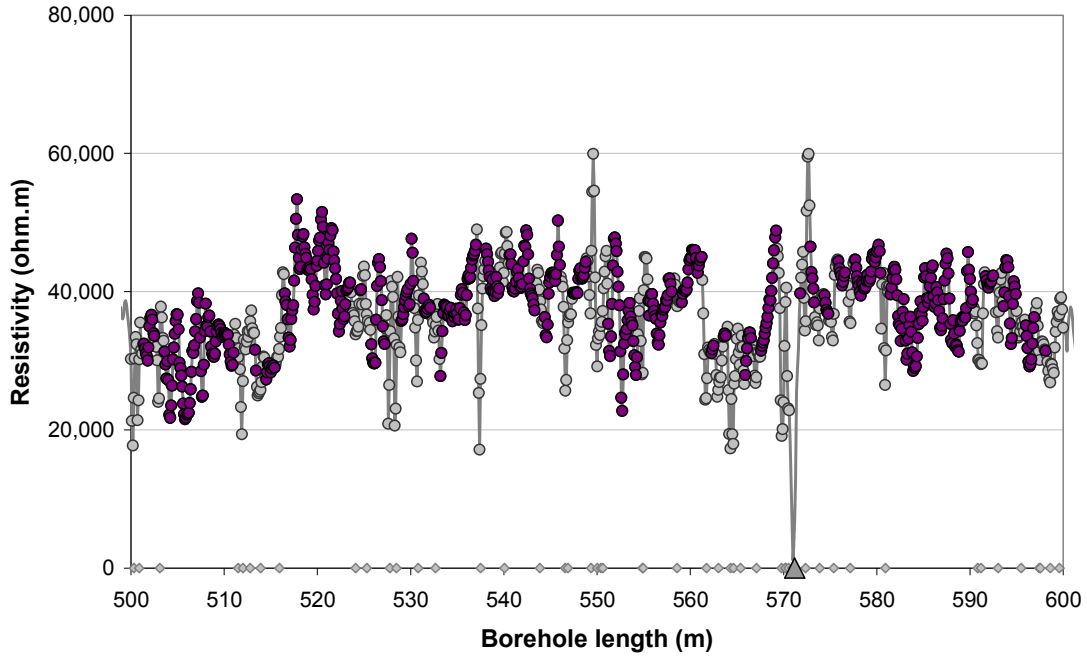

Rock resistivity
Fractured rock resistivity
Rock matrix resistivity
Location of broken fracture parting the drill core
Location of hydraulically conductive fracture detected in the difference flow logging

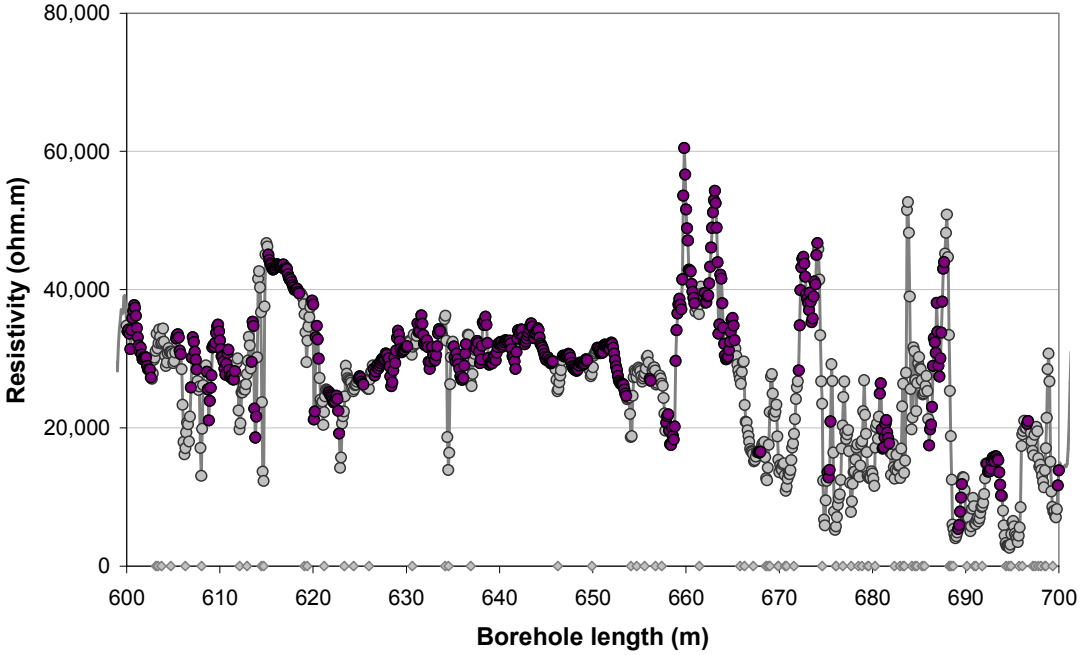

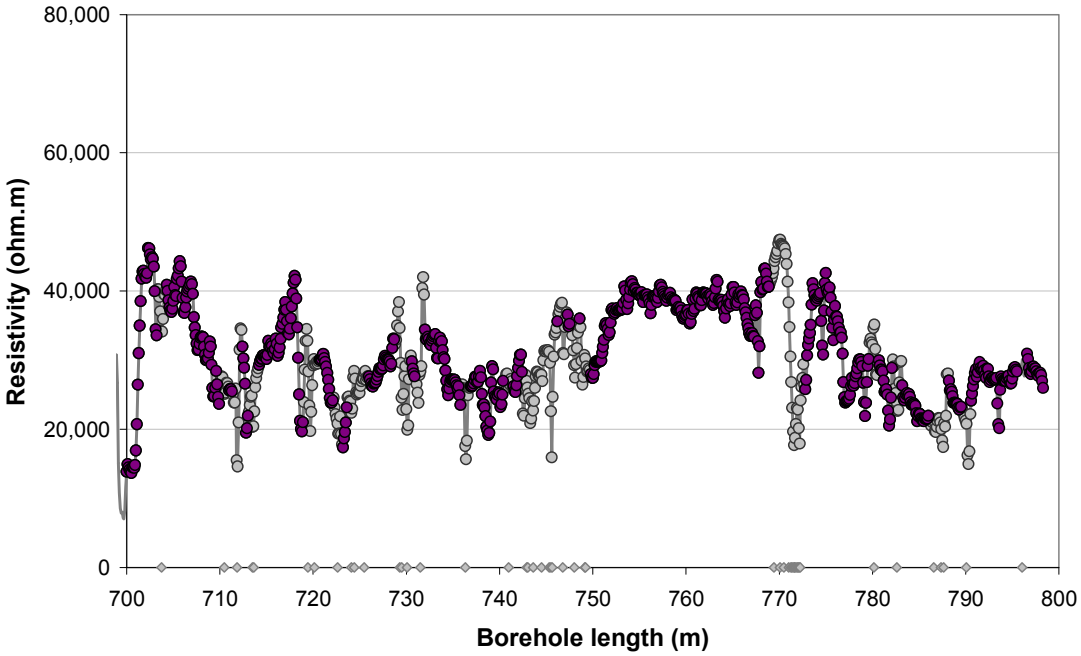

Rock resistivity
Fractured rock resistivity
Rock matrix resistivity
Location of broken fracture parting the drill core
Location of hydraulically conductive fracture detected in the difference flow logging

Appendix A2: In situ rock resistivities and fractures KFM08C

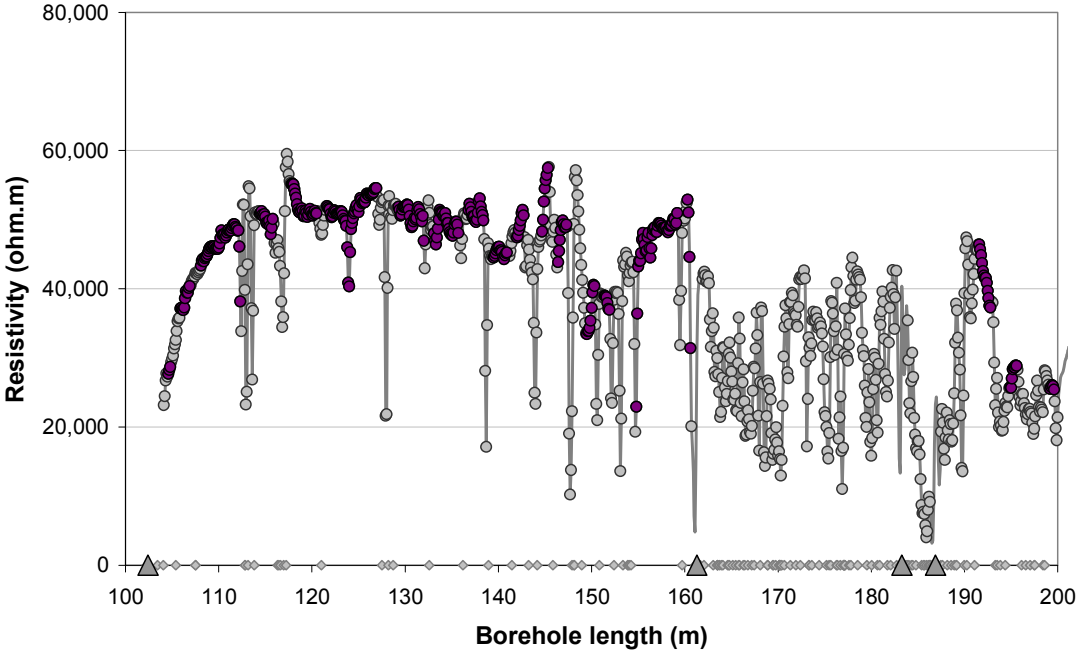

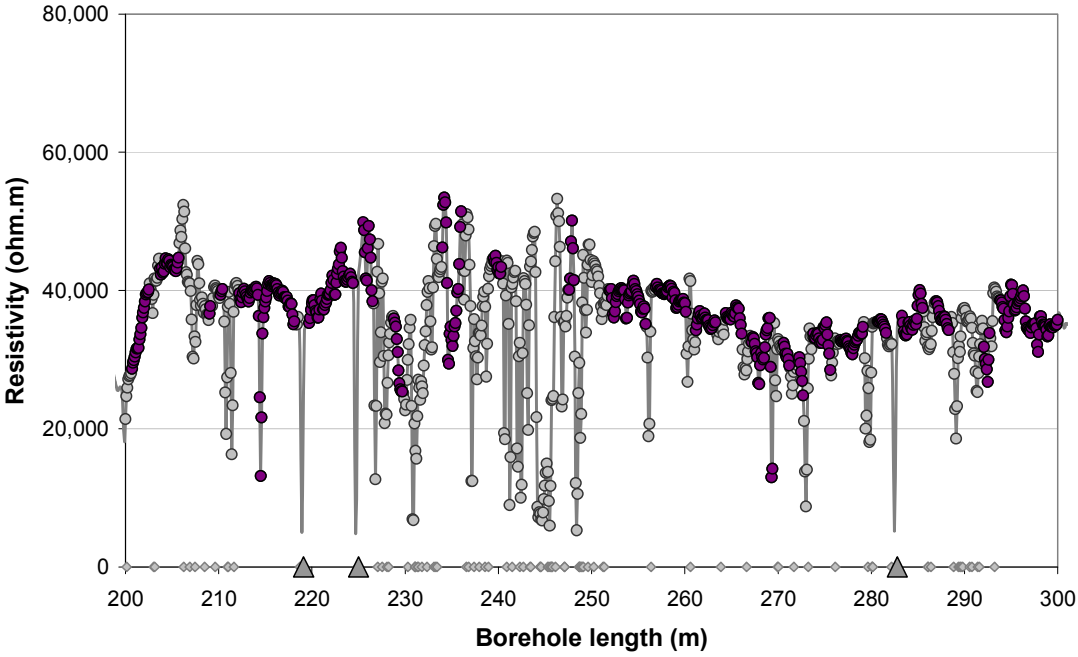

Rock resistivity
Fractured rock resistivity
Rock matrix resistivity
Location of broken fracture parting the drill core
Location of hydraulically conductive fracture detected in the difference flow logging

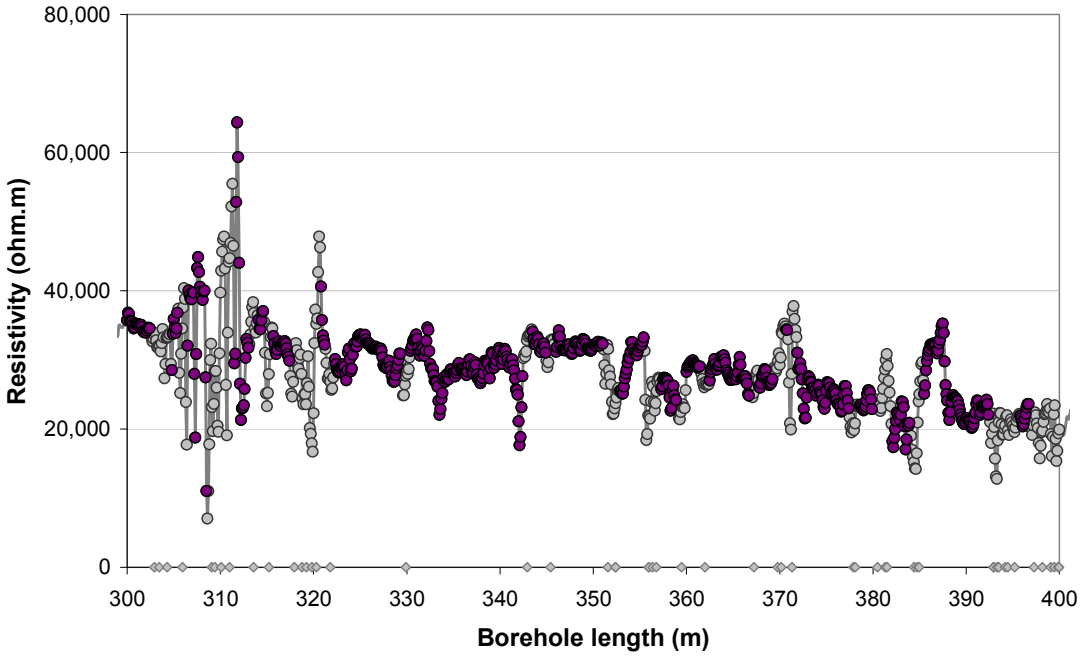

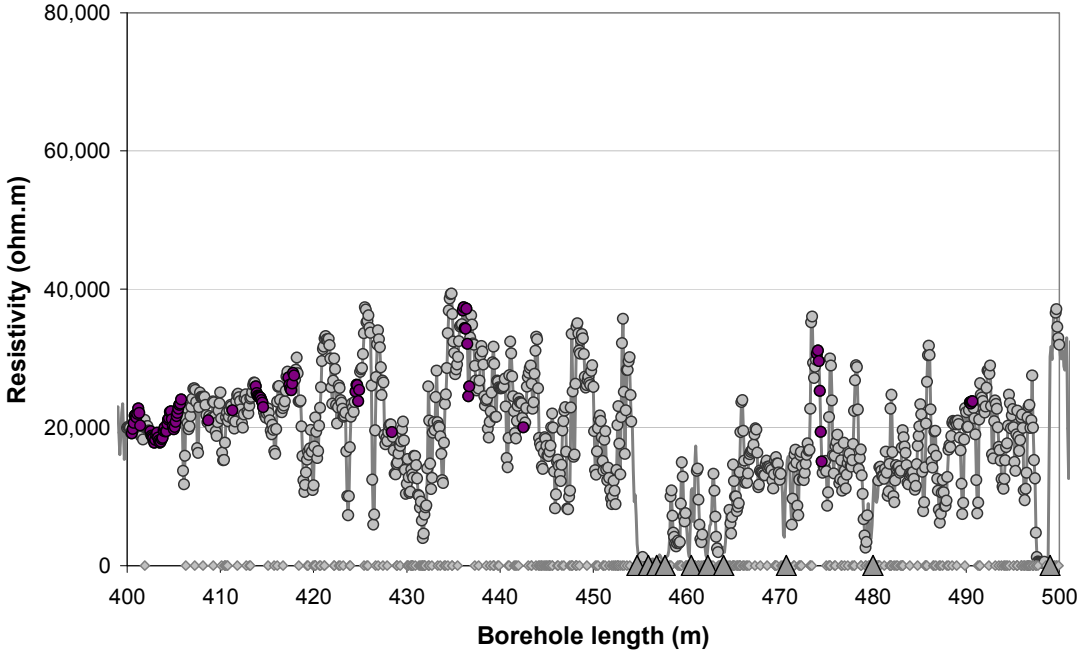

Rock resistivity
Fractured rock resistivity
Rock matrix resistivity
Location of broken fracture parting the drill core
Location of hydraulically conductive fracture detected in the difference flow logging

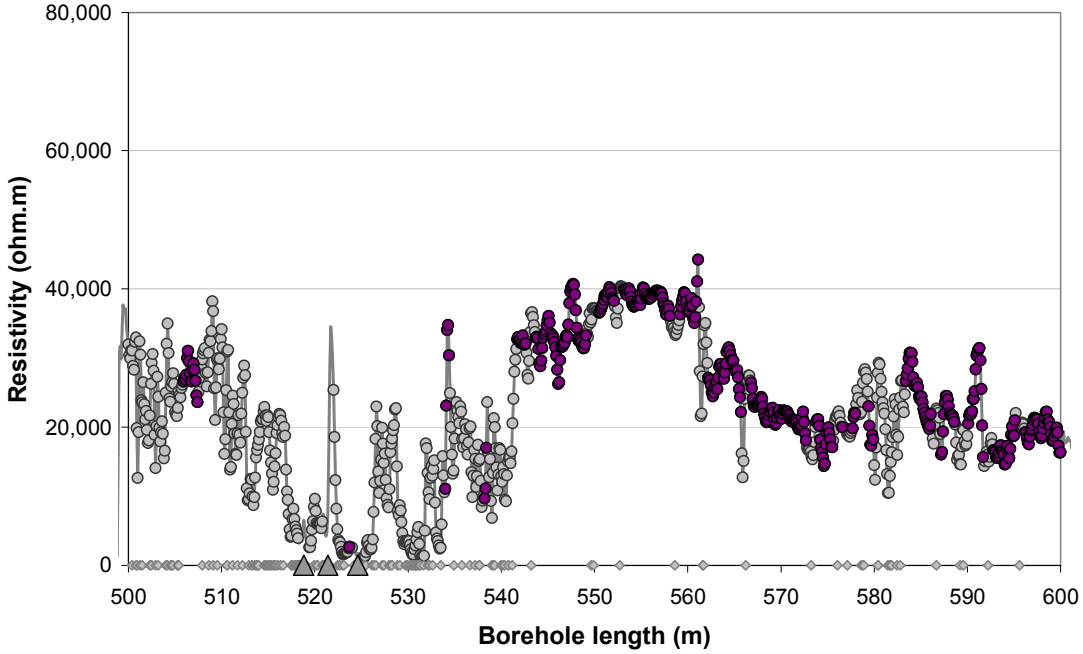

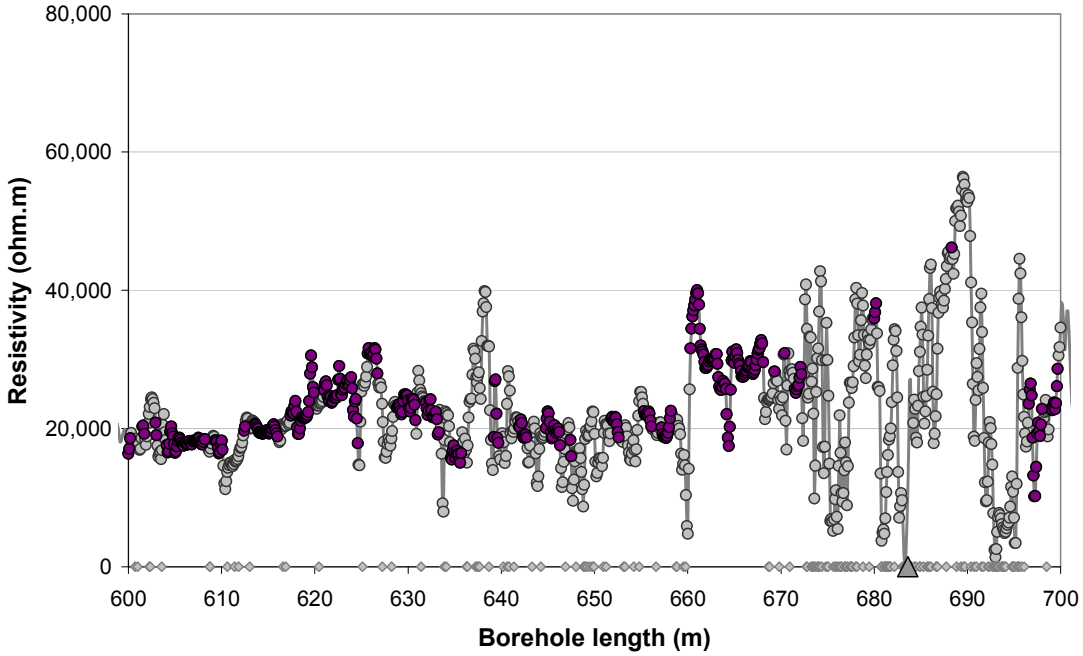

Rock resistivity
Fractured rock resistivity
Rock matrix resistivity
Location of broken fracture parting the drill core
Location of hydraulically conductive fracture detected in the difference flow logging

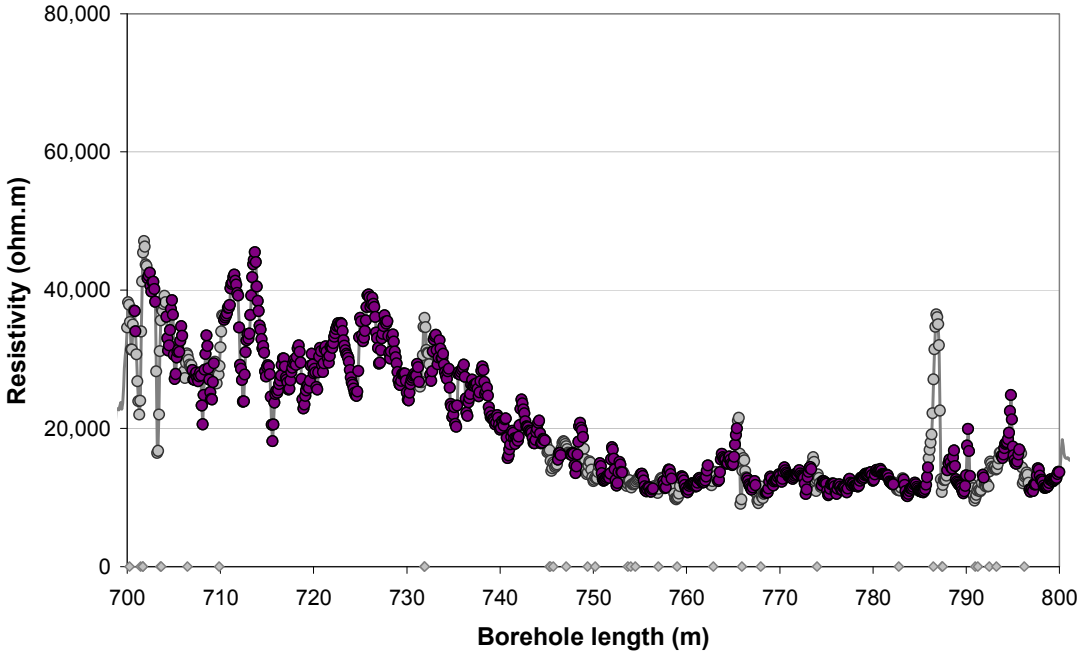

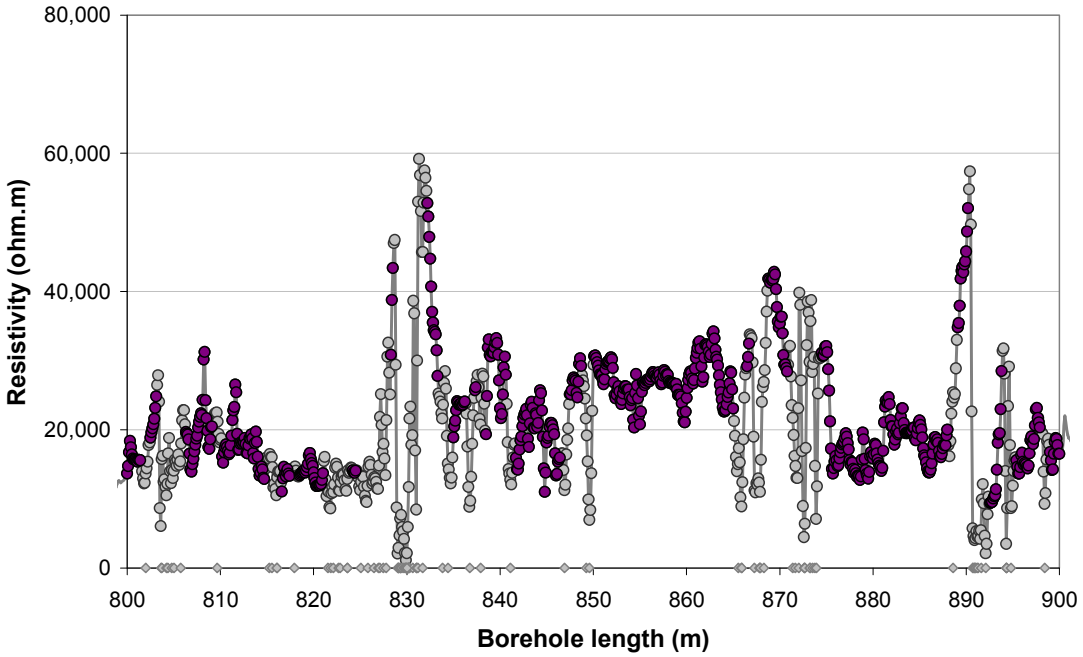

Rock resistivity
Fractured rock resistivity
Rock matrix resistivity
Location of broken fracture parting the drill core
Location of hydraulically conductive fracture detected in the difference flow logging

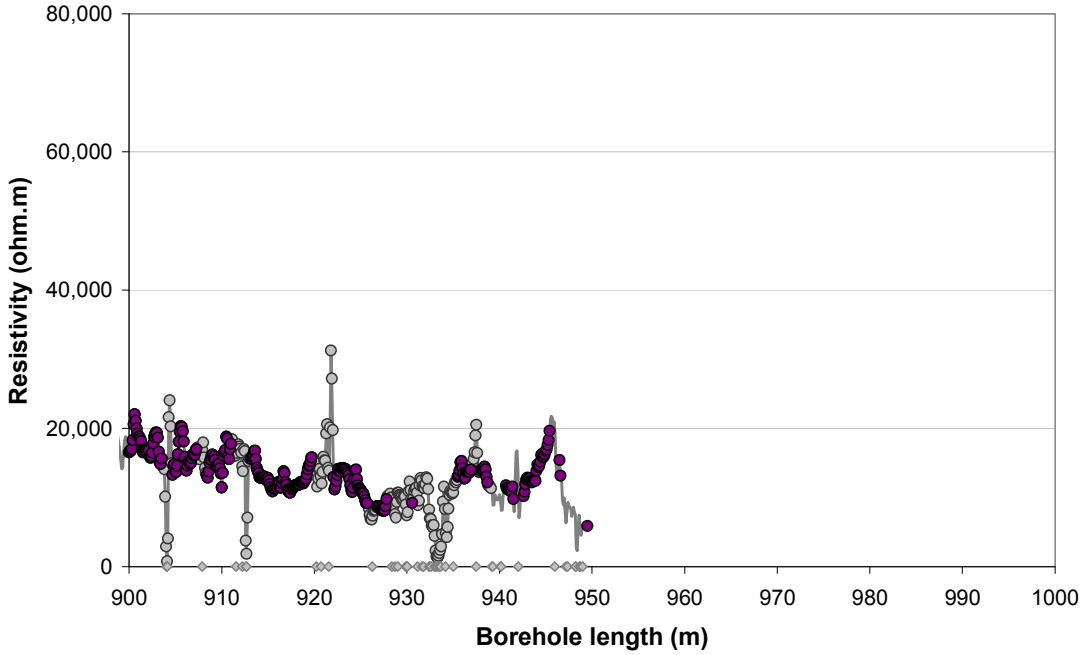

Rock resistivity
Fractured rock resistivity
Rock matrix resistivity
Location of broken fracture parting the drill core
Location of hydraulically conductive fracture detected in the difference flow logging

Appendix B1: In situ formation factors KFM01D

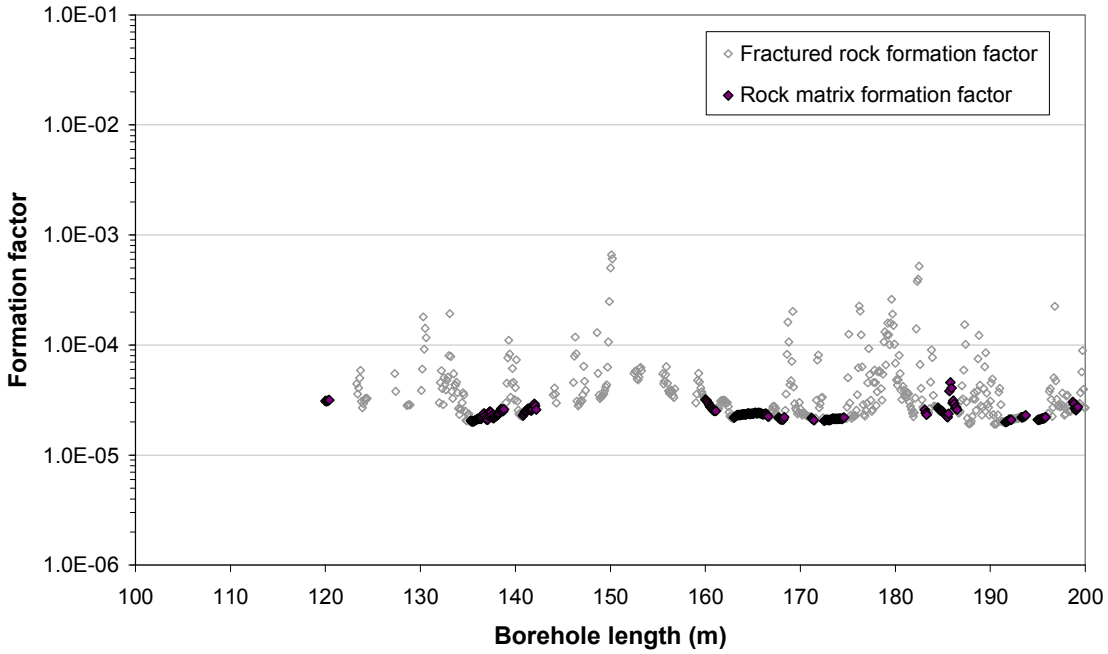

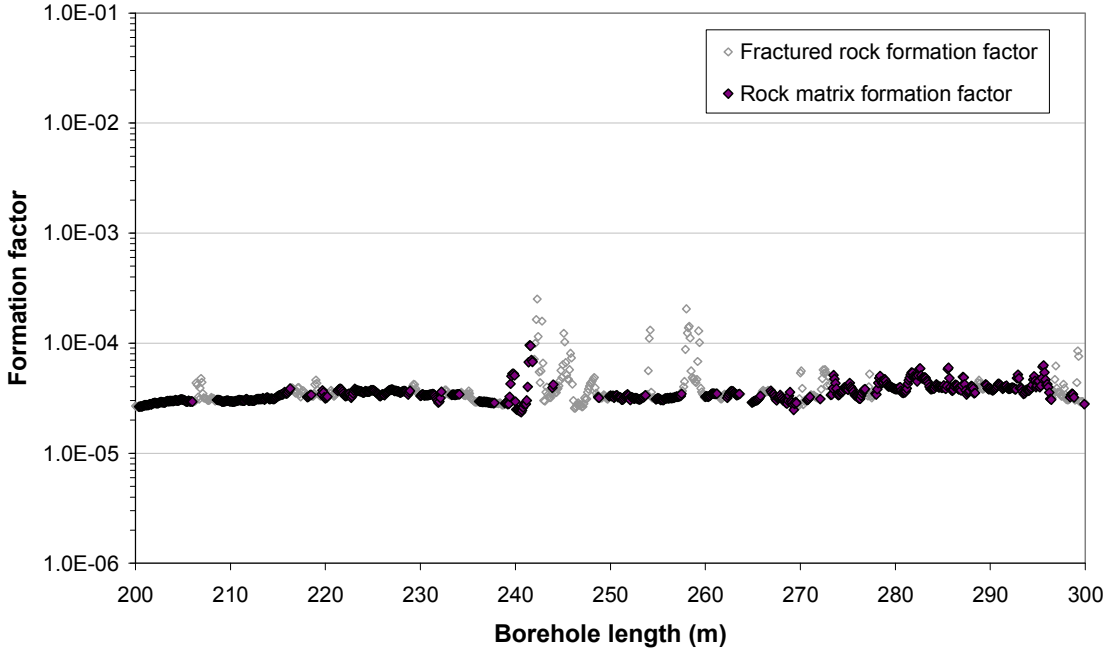

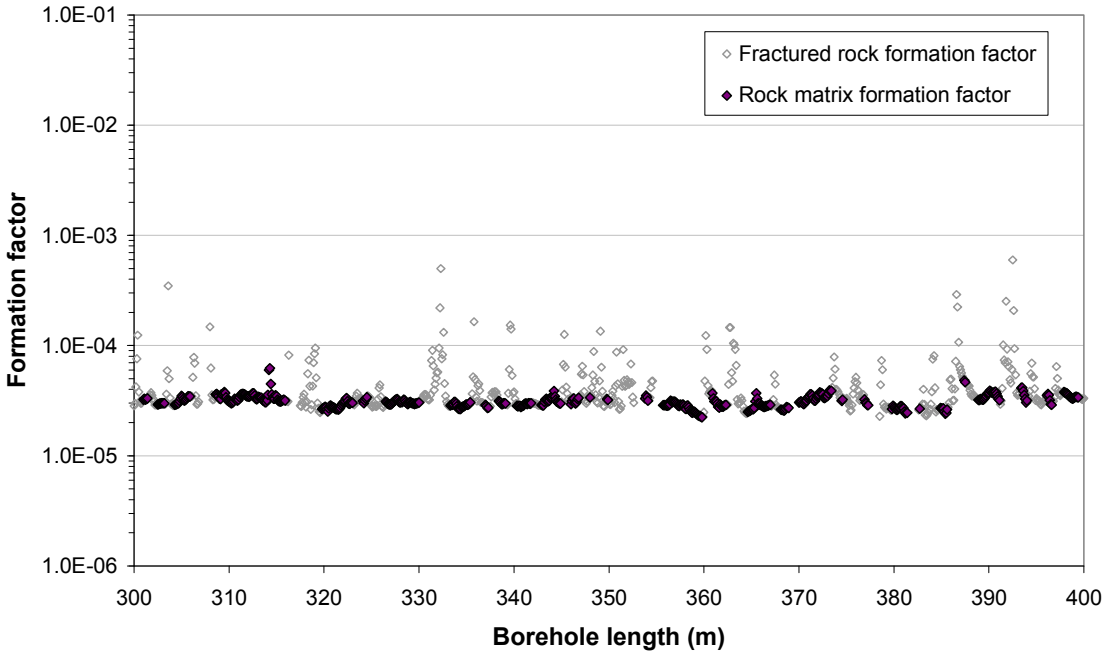
Fractured rock formation factor
Rock matrix formation factor
Formation factor
1.0E-01
1.0E-02
1.0E-03
1.0E-04
1.0E-05
1.0E-06
300
310
320
330
340
350
360
370
380
390
400
Borehole length (m)

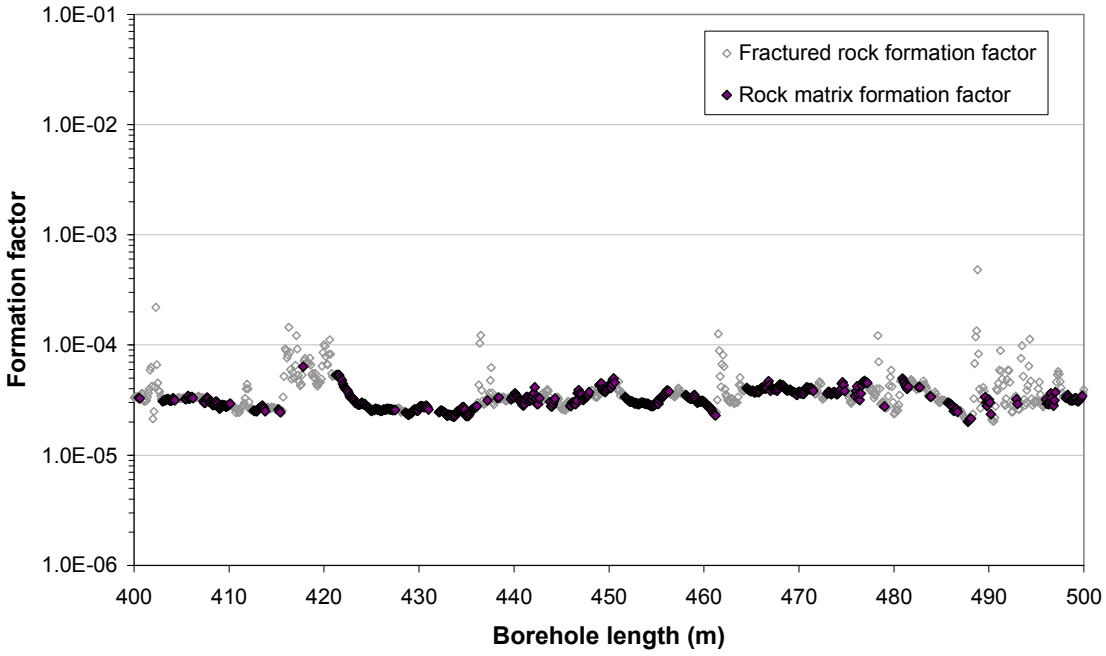
Fractured rock formation factor
Rock matrix formation factor
Formation factor
1.0E-01
1.0E-02
1.0E-03
1.0E-04
1.0E-05
1.0E-06
400
410
420
430
440
450
460
470
480
490
500
Borehole length (m)

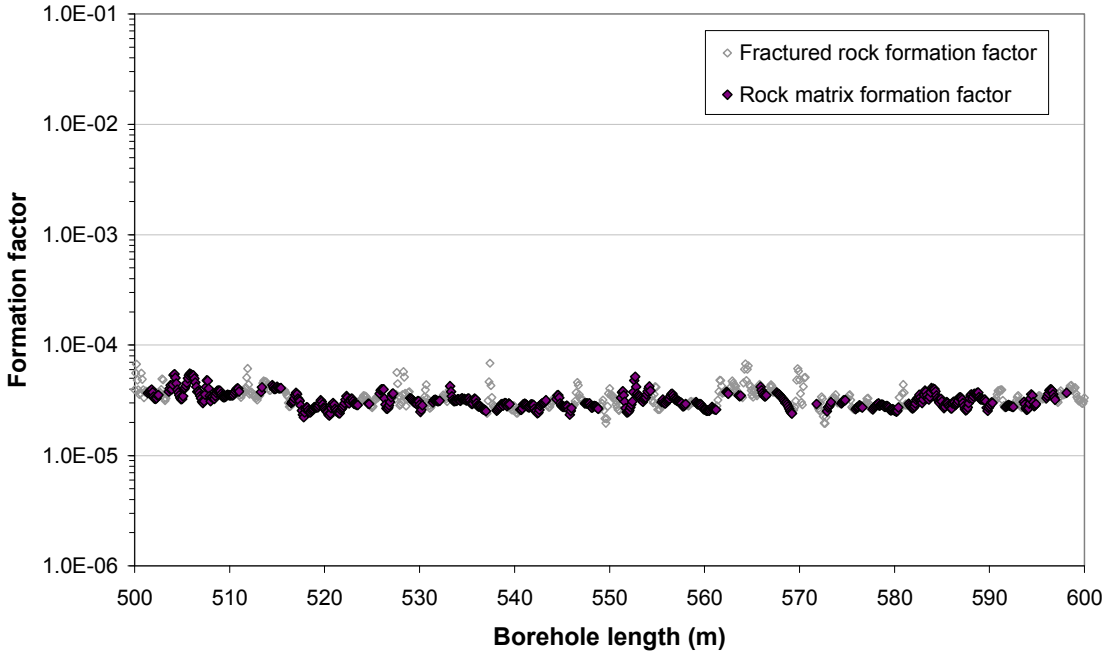
Fractured rock formation factor
Rock matrix formation factor
Formation factor
1.0E-01
1.0E-02
1.0E-03
1.0E-04
1.0E-05
1.0E-06
500
510
520
530
540
550
560
570
580
590
600
Borehole length (m)

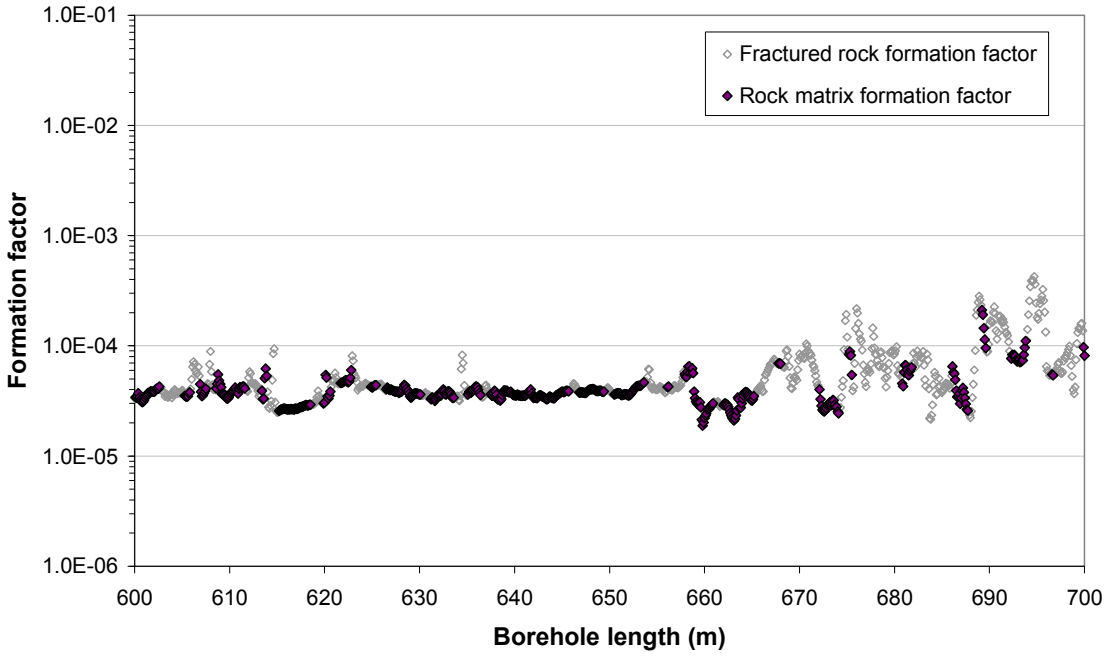
Fractured rock formation factor
Rock matrix formation factor
Formation factor
1.0E-01
1.0E-02
1.0E-03
1.0E-04
1.0E-05
1.0E-06
600
610
620
630
640
650
660
670
680
690
700
Borehole length (m)

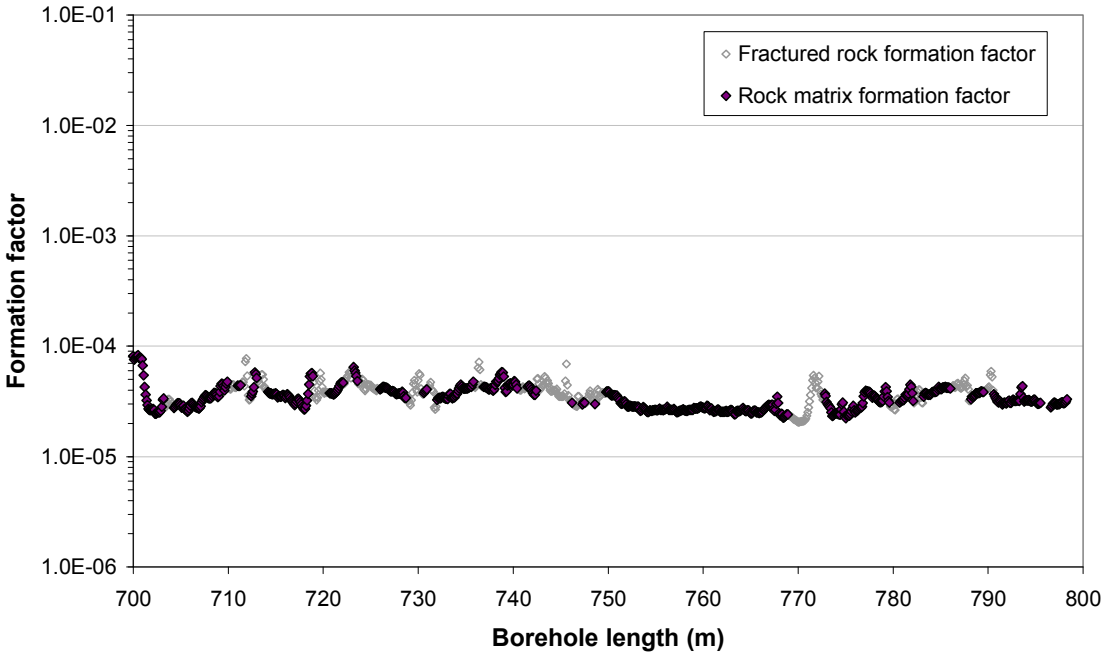
Fractured rock formation factor
Rock matrix formation factor
Formation factor
1.0E-01
1.0E-02
1.0E-03
1.0E-04
1.0E-05
1.0E-06
700
710
720
730
740
750
760
770
780
790
800
Borehole length (m)

Appendix B2: In situ formation factors KFM08C

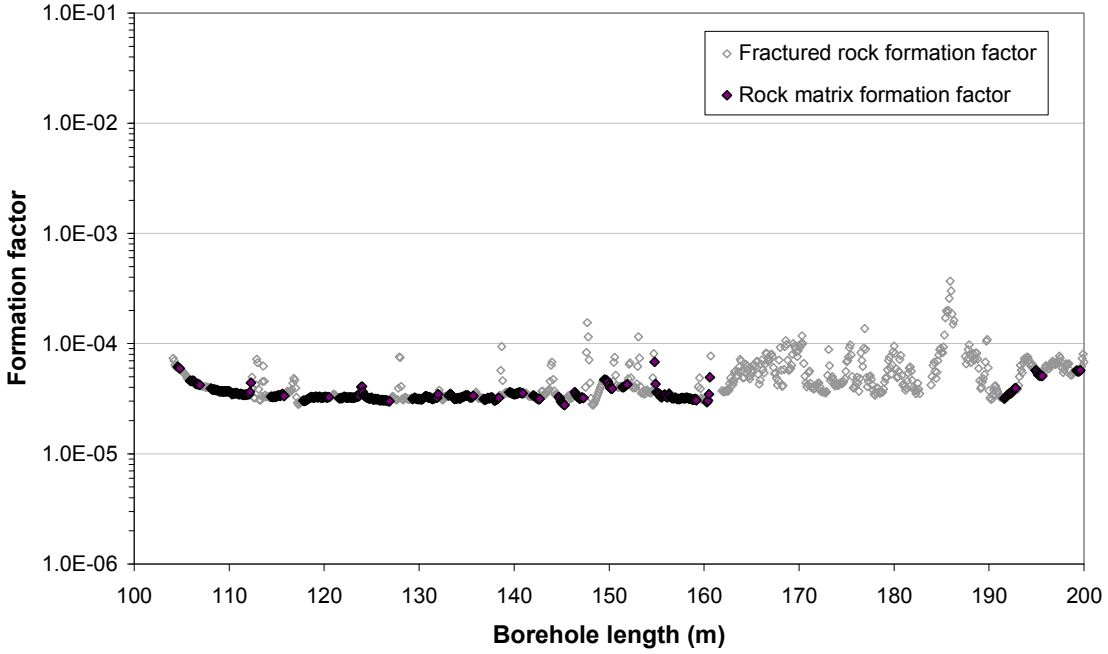

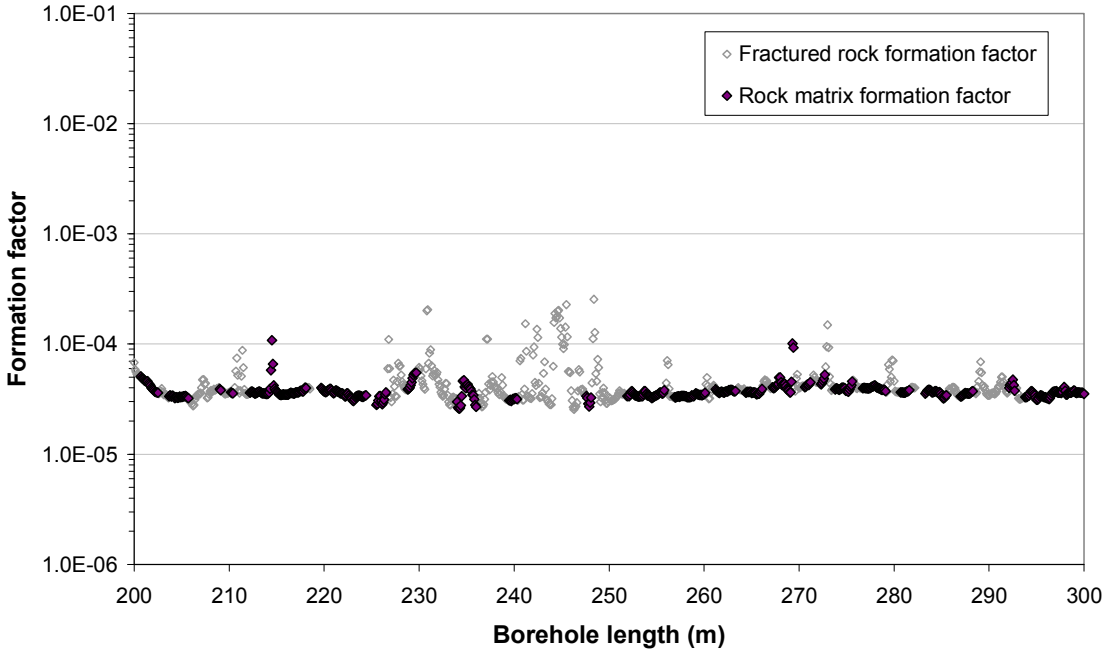

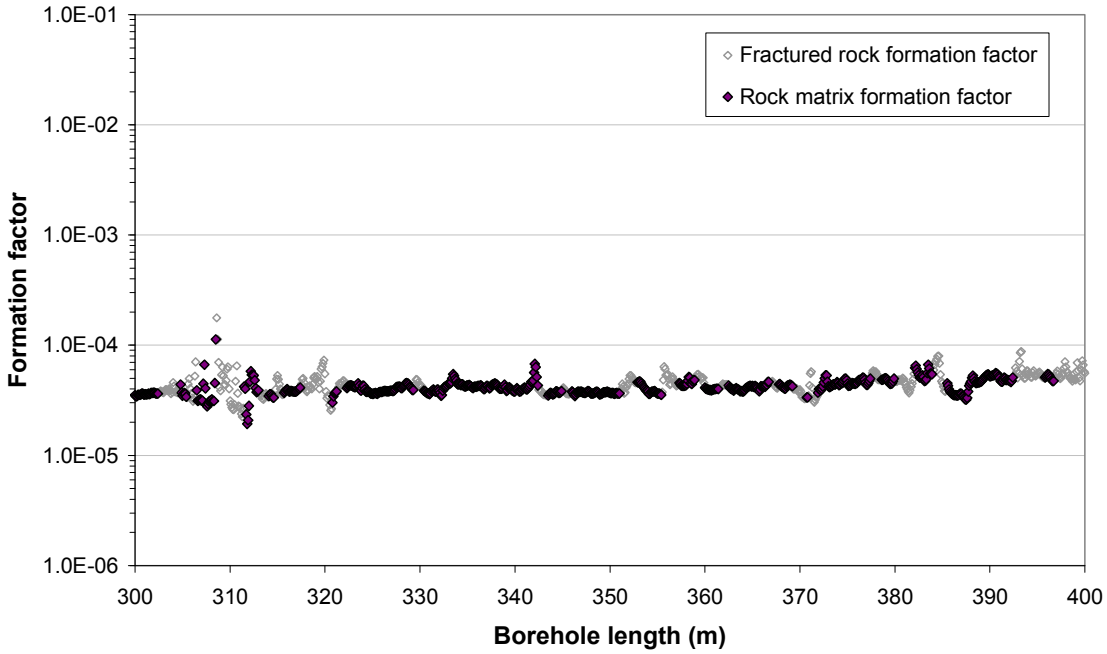
Fractured rock formation factor
Rock matrix formation factor
Formation factor
1.0E-01
1.0E-02
1.0E-03
1.0E-04
1.0E-05
1.0E-06
300
310
320
330
340
350
360
370
380
390
400
Borehole length (m)

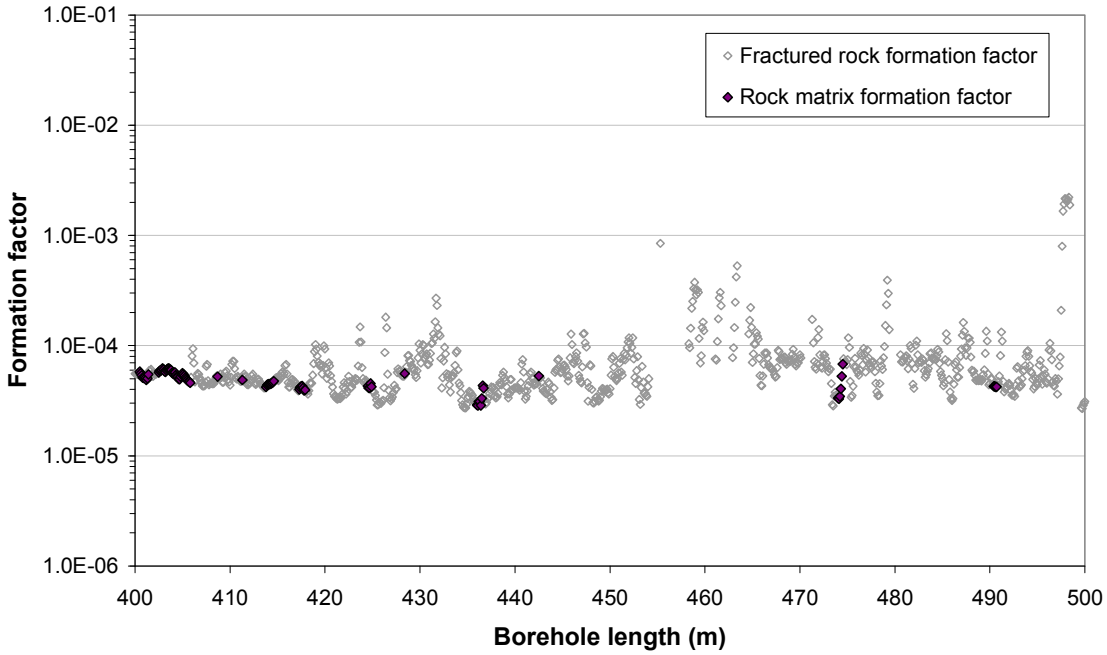
Fractured rock formation factor
Rock matrix formation factor
Formation factor
1.0E-01
1.0E-02
1.0E-03
1.0E-04
1.0E-05
1.0E-06
400
410
420
430
440
450
460
470
480
490
500
Borehole length (m)

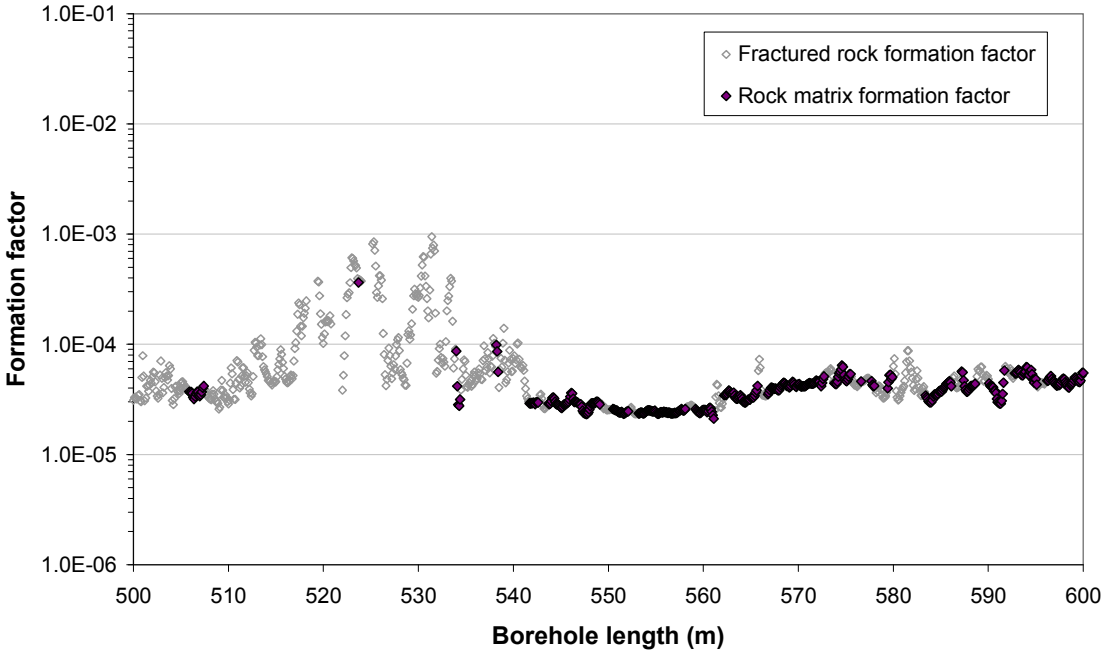
Fractured rock formation factor
Rock matrix formation factor
Formation factor
1.0E-01
1.0E-02
1.0E-03
1.0E-04
1.0E-05
1.0E-06
500
510
520
530
540
550
560
570
580
590
600
Borehole length (m)

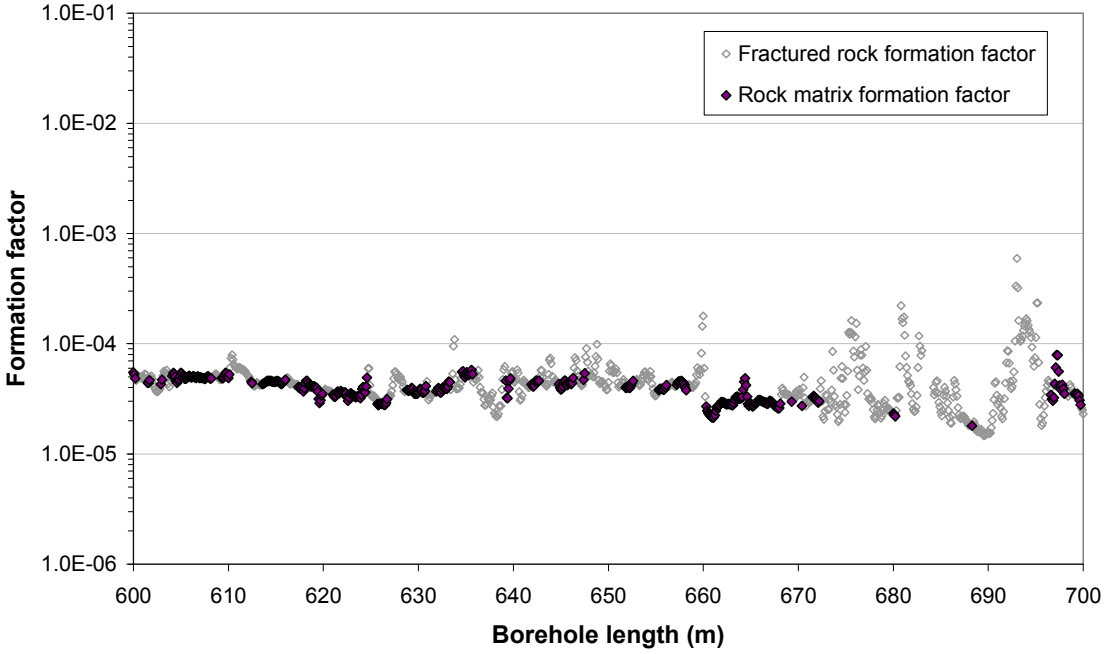
Fractured rock formation factor
Rock matrix formation factor
Formation factor
1.0E-01
1.0E-02
1.0E-03
1.0E-04
1.0E-05
1.0E-06
600
610
620
630
640
650
660
670
680
690
700
Borehole length (m)

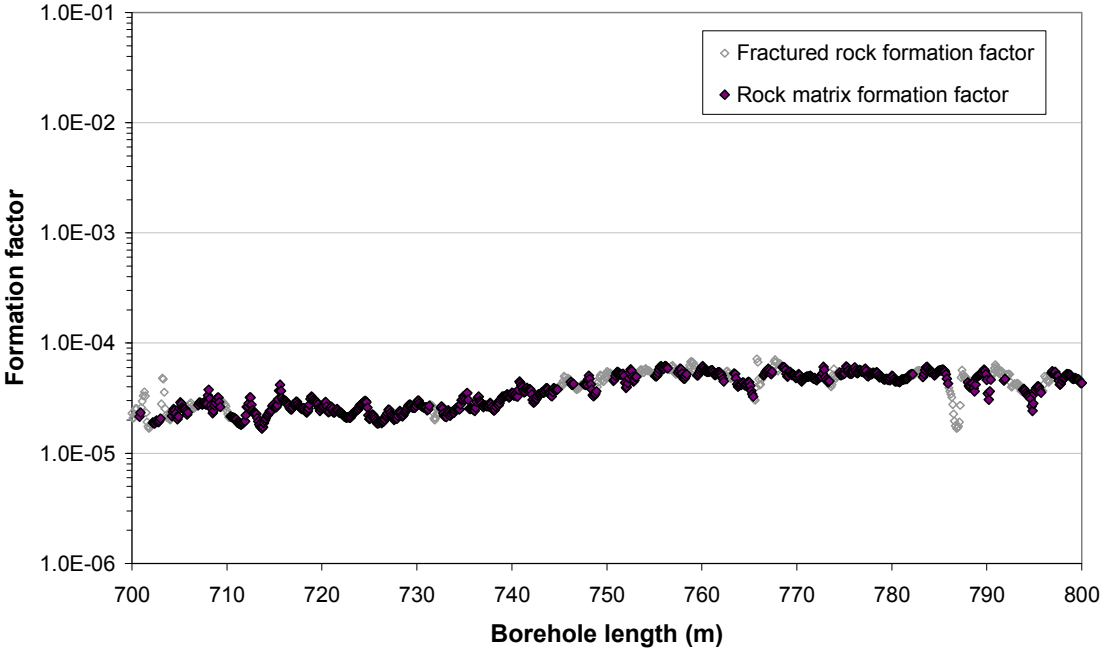
Fractured rock formation factor
Rock matrix formation factor
Formation factor
1.0E-01
1.0E-02
1.0E-03
1.0E-04
1.0E-05
1.0E-06
700
710
720
730
740
750
760
770
780
790
800
Borehole length (m)

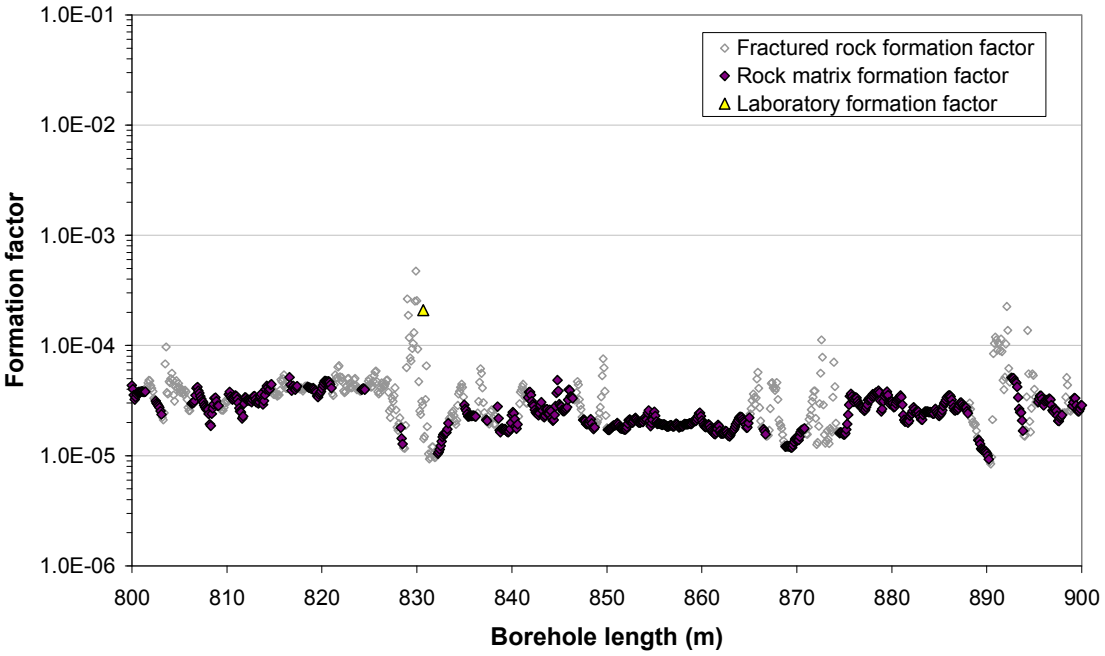
Fractured rock formation factor
Rock matrix formation factor
Laboratory formation factor
Formation factor
1.0E-01
1.0E-02
1.0E-03
1.0E-04
1.0E-05
1.0E-06
800
810
820
830
840
850
860
870
880
890
900
Borehole length (m)

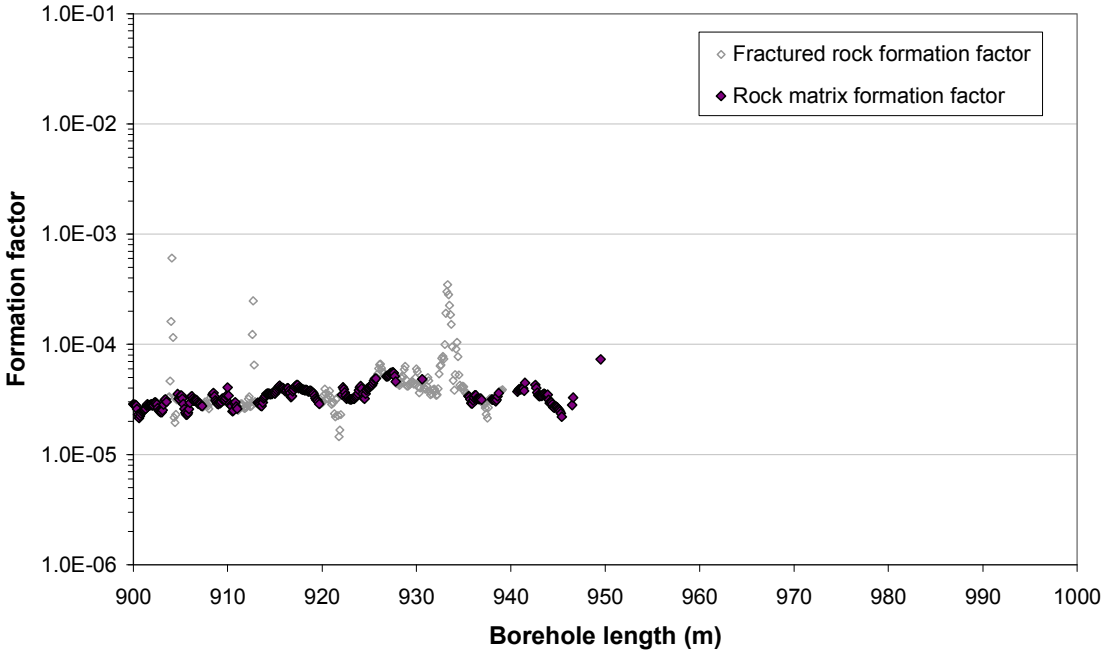
Fractured rock formation factor
Rock matrix formation factor
Formation factor
1.0E-01
1.0E-02
1.0E-03
1.0E-04
1.0E-05
1.0E-06
900
910
920
930
940
950
960
970
980
990
1000
Borehole length (m)

Appendix C

Chemmac indata for relation between EC and Cl^-

Only the last data points in time series (shaded) have been used in Figure 4-9.

Borehole	Secup (m)	Seclow (m)	Sample no.	Cl^- mg/l	EC (mS/m)	Source
KFM09A	785.10	792.24	12,239	14,600	3,690	Appendix 7, SKB P-06-217
KFM09A	785.10	792.24	12,241	14,800	3,700	
KFM09A	785.10	792.24	12,242	14,200	3,600	
KFM09A	785.10	792.24	12,243	14,800	3,720	
KFM09A	785.10	792.24	12,244	14,800	3,670	
KFM01D	428.50	435.64	12,307	5,370	1,510	Appendix 10, SKB P-06-227
KFM01D	428.50	435.64	12,314	5,460	1,540	
KFM01D	428.50	435.64	12,315	5,350	1,540	
KFM01D	428.50	435.64	12,316	5,160	1,500	
KFM01D	428.50	435.64	12,324	5,090	1,470	
KFM01D	428.50	435.64	12,326	4,940	1,420	
KFM01D	568.00	575.14	12,331	5,880	1,660	Appendix 10, SKB P-06-227
KFM01D	568.00	575.14	12,343	5,960	1,670	
KFM01D	568.00	575.14	12,350	5,890	1,670	
KFM01D	568.00	575.14	12,351	5,910	1,670	
KFM01D	568.00	575.14	12,354	5,800	1,640	
KFM01D	568.00	575.14	12,364	4,630	1,360	
KFM08A	683.50	690.64	8,963	6,190	1,700	Appendix 9, SKB P-06-63
KFM08A	683.50	690.64	8,965	6,180	1,710	
KFM08A	683.50	690.64	8,967	6,100	1,690	
KFM08A	683.50	690.64	8,968	6,010	1,700	
KFM08A	683.50	690.64	8,969	6,080	1,700	
KFM08A	683.50	690.64	8,978	6,070	1,690	
KFM08A	683.50	690.64	8,985	6,160	1,700	
KFM08A	683.50	690.64	8,987	6,090	1,690	
KFM08A	683.50	690.64	8,988	6,120	1,700	
KFM08A	683.50	690.79	8,989	6,030	1,690	
KFM08A	683.50	690.79	8,990	6,140	1,700	
KFM08A	683.50	690.64	8,991	6,170	1,700	
KFM08A	683.50	690.64	12,000	6,100	1,690	
KFM04A	230.50	237.64	8,154	5,480	1,670	Appendix 8, SKB P-04-109
KFM04A	230.50	237.64	8,155	5,490	1,620	
KFM04A	230.50	237.64	8,156	5,510	1,610	
KFM04A	230.50	237.64	8,160	5,550	1,630	
KFM04A	230.50	237.64	8,267	5,580	1,620	
KFM04A	230.50	237.64	8,269	5,680	1,610	
KFM04A	354.00	361.13	8,283	5,610	1,660	Appendix 8, SKB P-04-109
KFM04A	354.00	361.13	8,286	5,780	1,660	
KFM04A	354.00	361.13	8,287	5,780	1,660	
KFM03A	386.00	391.00	4,983	5,440	1,600	Appendix 12, SKB P-04-108
KFM03A	386.00	391.00	8,008	5,420	1,610	
KFM03A	386.00	391.00	8,011	5,440	1,590	
KFM03A	386.00	391.00	8,012	5,450	1,670	

KFM03A	448.00	453.00	8,015	5,380	1,620	Appendix 12, SKB P-04-108
KFM03A	448.00	453.00	8,017	5,430	1,600	
KFM03A	448.50	455.62	8,282	5,440	1,590	
KFM03A	448.50	455.62	8,284	5,330	1,580	
KFM03A	639.00	646.12	8,265	5,380	1,600	Appendix 12, SKB P-04-108
KFM03A	639.00	646.12	8,268	5,380	1,530	
KFM03A	639.00	646.12	8,270	5,470	1,540	
KFM03A	639.00	646.12	8,271	5,440	1,690	
KFM03A	639.00	646.12	8,273	5,430	1,620	
KFM03A	939.50	946.62	8,275	7,560	2,060	Appendix 12, SKB P-04-108
KFM03A	939.50	946.62	8,276	7,830	2,110	
KFM03A	939.50	946.62	8,277	7,930	2,170	
KFM03A	939.50	946.62	8,278	8,150	2,040	
KFM03A	939.50	946.62	8,279	8,330	1,970	
KFM03A	939.50	946.62	8,280	8,480	1,890	
KFM03A	939.50	946.62	8,281	8,560	1,990	
KFM03A	980.00	1,001.19	8,096	10,000	2,640	Appendix 12, SKB P-04-108
KFM03A	980.00	1,001.19	8,098	9,990	2,760	
KFM03A	980.00	1,001.19	8,101	9,950	2,670	
KFM03A	980.00	1,001.19	8,103	9,890	2,630	
KFM03A	980.00	1,001.19	8,104	9,890	2,670	
KFM03A	980.00	1,001.19	8,105	9,740	2,650	
KFM03A	980.00	1,001.19	8,151	9,720	2,660	
KFM03A	980.00	1,001.19	8,152	9,690	2,560	
KFM06A	266.00	271.00	8,860	5,190	1,520	Appendix 9, SKB P-05-178
KFM06A	353.50	360.62	8,802	4,710	1,400	Appendix 9, SKB P-05-178
KFM06A	353.50	360.62	8,803	4,620	1,370	
KFM06A	353.50	360.62	8,804	4,580	1,360	
KFM06A	353.50	360.62	8,806	4,600	1,360	
KFM06A	353.50	360.62	8,807	4,570	1,340	
KFM06A	353.50	360.62	8,808	4,570	1,360	
KFM06A	353.50	360.62	8,809	4,560	1,350	
KFM06A	353.50	360.62	8,838	4,850	1,360	
KFM06A	768.00	775.12	8,746	6,730	1,870	Appendix 9, SKB P-05-178
KFM06A	768.00	775.12	8,747	6,830	1,920	
KFM06A	768.00	775.12	8,748	7,040	1,960	
KFM06A	768.00	775.12	8,749	7,050	1,970	
KFM06A	768.00	775.12	8,781	7,000	1,970	
KFM06A	768.00	775.12	8,782	7,150	1,970	
KFM06A	768.00	775.12	8,783	6,940	1,980	
KFM06A	768.00	775.12	8,784	6,840	1,980	
KFM06A	768.00	775.12	8,785	7,080	1,990	